NEUTRONIC ANALYSIS FOR THE UVAR REACTOR HEU TO LEU CONVERSION PROJECT

A Thesis

Presented to

the Faculty of the School Engineering and Applied Science

University of Virginia

In Partial Fulfillment

of the Requirements for the Degree

Master of Science

by

David W. Freeman

July, 1989

ACKNOWLEDGEMENT

This work was performed with support from Department of Energy Grants

#DEFG0588ER75388
and
#DEFG0586ER75273

ABSTRACT

The University of Virginia Research Reactor is currently in the process of converting from high-enriched uranium (HEU) fuel to low-enriched uranium (LEU) fuel. The conversion is in response to a mandate from the Nuclear Regulatory Commission. This thesis addresses several neutronics concerns associated with the conversion project including: 1) control rod worths; 2) radial peaking factors; 3) temperature feedback effects; 4) moderator void feedback effects; 5) reflector worth effects; 6) delayed neutron fractions; and 7) prompt neutron lifetimes.

Control rod reactivity worths for LEU fueled cores were found to be essentially the same as for the HEU fueled cores. Radial peaking factors for the LEU fuel were found to be slightly higher than for HEU fuel due to the harder flux spectrum associated with the LEU fuel. Temperature and moderator void reactivity feedback effects for both the LEU and HEU fueled cores were found to be very similar except for the doppler effect which was significantly higher in the LEU fuel due to the higher uranium-238 loading.

Reflector worths for several different water and graphite reflector options were quantified for the LEU fueled cores, and heavy water reflector tanks were analyzed. An effective delayed neutron fraction of 0.0074 was determined for both the HEU and LEU fueled cores. A prompt neutron lifetime of 67 micro-seconds was determined for the LEU core which was about 15 percent lower than

that determined for the HEU core.

The overall thesis results show that the LEU-fueled core will behave very similarly to the HEU core currently being used.

ACKNOWLEDGEMENTS

This report is dedicated to my wife, Donna, and my daughters, Sarah and Jodi, who constantly supported me throughout the project.

Thanks go to Dr. Rydin for providing guidance and keeping the project on track. A special thanks goes to Vicki Thomas who typed this thesis and helped with the format.

Thanks go to Press Farrar who provided historical background and documentation for the reactor.

Finally, thanks are owed to Mary Fehr and Stuart Wasserman for laying the strong foundation of computer models which I inherited.

TABLE OF CONTENTS

LIST OF FIGURES

LIST OF TABLES

CHAPTER 1. INTRODUCTION

This report presents several studies designed to address neutronics issues and concerns associated with converting the University Of Virginia Research Reactor (UVAR) from highly-enriched uranium (HEU) fuel to low-enriched uranium (LEU) fuel. The neutronics studies were performed using advanced neutronics computer modeling techniques. Studies presented in this report address the following topics: 1) control rod worths; 2) radial peaking factors; 3) temperature and moderator feedback effects; 4) reflector worths; and 5) delayed neutron and prompt neutron lifetimes. Background information used to build the computer models and study methodologies are also addressed.

Several research reactor facilities in the United States use HEU fuel. The Nuclear Regulatory Commission (NRC) has directed all research facilities using HEU fuel to convert to LEU fuel. HEU fuels are often enriched in excess of 90 percent uranium-235 while LEU fuels have an enrichment limit of 20 percent. The order to convert to LEU fuel was in response to security and safeguards issues raised over the HEU fuel.

Currently, the UVAR is in the process of being converted from HEU to LEU fuel. The conversion process is being performed by the UVAR staff and is non-trivial. The process includes: 1) a revision of the Safety Analysis Report; 2) Technical

Specifications changes; and 3) other, as yet undefined, analyses deemed necessary by NRC.

To date, much work has been performed on the project by both UVAR staff and graduate students. This work is well summarized in the facility Progress Report [1] to the Department of Energy (DOE). The work has focused on the operating performance of the LEU fuel as compared to the currently used HEU fuel.

LEU fuel elements considered for use in the UVAR will use generic LEU fuel plates described in Chapter 2. LEU fuel elements using 18 plates (LEU-18), 20 plates (LEU-20), and 22 plates (LEU-22) have been considered as potential replacements for the current 18 plate HEU fuel elements (HEU-18). The neutronics analyses have not addressed LEU-20 fuel elements and have assumed that their characteristics were bounded by the LEU-18 and LEU-22 fuel element characteristics.

In the fall of 1988, The University of Virginia (UVA) Reactor Safety Committee tentatively approved the use of either the LEU-18, LEU-20, or LEU-22 fuel elements. Work performed by Fehr [2] showed that the LEU-22 fuel element would be a superior replacement for the current fuel in terms of core lifetime. Based on this information, the UVAR staff decided to choose LEU-22 fuel as the preferred replacement element. For this reason, several of the studies presented in this analysis address only the LEU-22 fuel option.

A key issue of concern was whether or not the UVAR control rods would provide an adequate reactivity insertion in LEU cores for safe operation and whether their associated reactivity effects would be significantly altered from those in HEU cores. This issue is addressed in Chapter 4 of this thesis and in Reference [3].

The focus of the HEU to LEU conversion safety analysis is the thermal hydraulics analysis [4]. This effort is supported by information presented in the peaking factor study presented in Chapter 5.

Chapter 6 presents a study which addresses temperature and moderator feedback effects for the LEU fuel, and Chapter 7 addresses reflector worth behavior for the various fuel options.

NRC informally requested, via a guidance handout at the 1988 National Organization of Test, Research, and Training Reactors (TRTR) meeting, that delayed neutron fractions and prompt neutron lifetimes be calculated as part of the license renewal process. The study presented in Chapter 8 addresses this issue.

It should be noted that no simple mechanism exists for quantifying errors associated with the computer modeling techniques used throughout this thesis. Errors may be incurred in the modeling process, computer computations, and input data. A default error value of plus or minus 5 percent has been chosen as representing what is believed to be a reasonable estimate of the error involved with values presented in this thesis. Higher error estimates are quoted in this thesis when deemed appropriate. As discussed in Chapter 9, the computer models can be "fine-tuned" when experimental data from the new LEU core becomes available. This process should eventually provide information allowing a better estimate of computational errors to be made.

The current schedule for the conversion project includes the submission of a revised Safety Analysis Report (in which the author will be heavily involved) in August, 1989. LEU fuel element fabrication is projected for completion by the end of 1989. Assuming that NRC licensing concerns can be addressed in a timely fashion, it should be possible to convert the UVAR to LEU fuel in early 1990.

2.0 BACKGROUND INFORMATION

This chapter presents background information which forms the basis for the UVAR neutronics models developed for analyses presented in this report. Presented below are descriptions of: 1) the UVAR reactor; 2) control rods; 3) HEU fuel; and 4) LEU fuel.

2.1 Description of the UVAR Reactor

The UVAR reactor is a pool type research reactor constructed in 1959. Currently licensed to operate at 2 megawatts, the UVAR is used primarily as a research tool. Research activities, such as neutron activation analysis and neutron radiography, use the reactor core as a powerful neutron source. The reactor assembly is comprised of fuel elements, control rod fuel elements, control rods, and graphite reflector elements; all of which sit in the reactor grid plate. The grid plate assembly is supported by an aluminum framework which is suspended from a movable bridge. Pool water (light water) serves as moderator, coolant, reflector, and radiation shielding.

The reactor sits under about 20 feet of water at the bottom of a 75,000 gallon pool. The reactor is cooled by pool water downflow through the core elements in excess of 1000 gallons per minute. This water passes through a tube-in-shell heat exchanger and is returned to the pool. Heat is transferred to the atmosphere via a cooling tower mounted on the facility roof.

A full description of the UVAR is presented in the facility Safety Analysis Report [5]. Certain key features of the UVAR, such as the grid plate and core components, are discussed below.

<u>Grid Plate</u>

The UVAR reactor is located on the reactor grid plate. The reactor is "built" by loading various core components into the grid plate to achieve a desired core configuration. Core configurations are widely varied and are limited only by shutdown margin and excess reactivity requirements.

The UVAR grid plate, shown in Figure 2-1, contains an 8-by-8 array of holes, approximately 2 1/2 inches in diameter, for positioning reactor components. For the purposes of this analysis, the grid plate has been subdivided into 64 equal grid cells measuring 3.189 inches by 3.031 inches [6]. The grid cells are depicted in Figure 2-1 with dotted lines.

<u>Reactor Core Components</u>

Reactor components include fuel elements, control rod fuel elements, graphite elements, and grid plate plugs. Reactor components are designed to fit into the grid plate holes and extend no further than the grid cell boundaries.

Fuel elements, control rod elements, and graphite elements all have similar dimensions of about 3 inches in length and width, and 35 inches in height. The bottom of each element consists of a cylindrical tapered nozzle which fits snugly into the grid plate

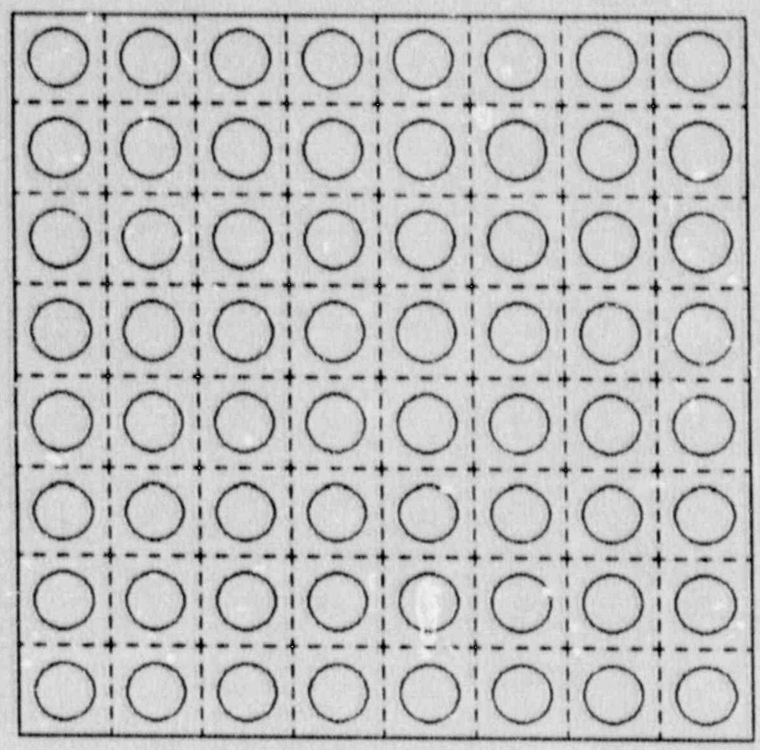

Figure 2-1. UVAR Grid Plate

holes. Graphite elements, used as reflectors, are generally placed on the outside faces of the fuel that makes up the core to enhance core reactivity.

Grid plugs are used to prevent water flow through empty grid locations. UVAR Standard Operating Procedures (SOPs) require all unused grid locations to be plugged in order to minimize non-element by-pass flow. A grid plug is a short metal cylinder, approximately 3 inches in diameter, mounted on a tapered nozzle. When inserted in the grid plate, the plug extends only a few inches above the grid plate, which is below the active fuel region.

2.2 Control Rods

The UVAR uses four control rods; 3 safety rods and 1 regulating rod. Safety rod reactivity worths range from 3 to 5% $\Delta\rho$ and are used to scram the reactor. The regulating rod has a relatively low worth (0.3-1% $\Delta\rho$) and is used primarily to compensate for small changes in reactivity. The control rods are oval and fit into the center hole of the control rod element. Each type of rod is discussed below.

<u>Safety Rods</u>

The UVAR safety rods are made of boron-stainless steel, clad in aluminum, and are about 1.5% natural boron by volume. The rods are about 25 inches long and have an oval cross section geometry with approximate dimensions of 2 1/4 by 7/8 inches. The rods are vertically grooved to increase surface area. The safety rods are magnetically coupled to their drive mechanisms and drop by gravity into the core on a scram signal.

Regulating Rod

The regulating rod, commonly referred to as the "reg rod", is made of stainless steel, clad in aluminum. It has the same dimensions as the safety rods but is not grooved. The rod is permanently attached to its drive mechanism and, therefore, does not drop on a scram signal. The reg rod has a relatively low worth and is generally located in the outer portions of the core, with the primary purpose of compensating for small reactivity changes associated with normal operations.

2.3 HEU Fuel

The UVAR is currently fueled with highly enriched uranium (HEU) fuel elements, shown in Figure 2-2. Each fuel element contains 18 curved fuel plates and is referred to as "HEU-18" fuel throughout this analysis. Each element initially contained 195 grams of U-235; however, the HEU fuel used in this analysis was partially burned, having an estimated 192.3 grams of U-235 per element. The element has approximate cross sectional dimensions of 3-by-3 inches, with an active fuel length of about 24 inches.

HEU control rod fuel elements are similar to the regular fuel elements except that the center 9 fuel plates have been removed to allow room for the control rod to move up and down. The HEU control rod element is shown in Figure 2-2.

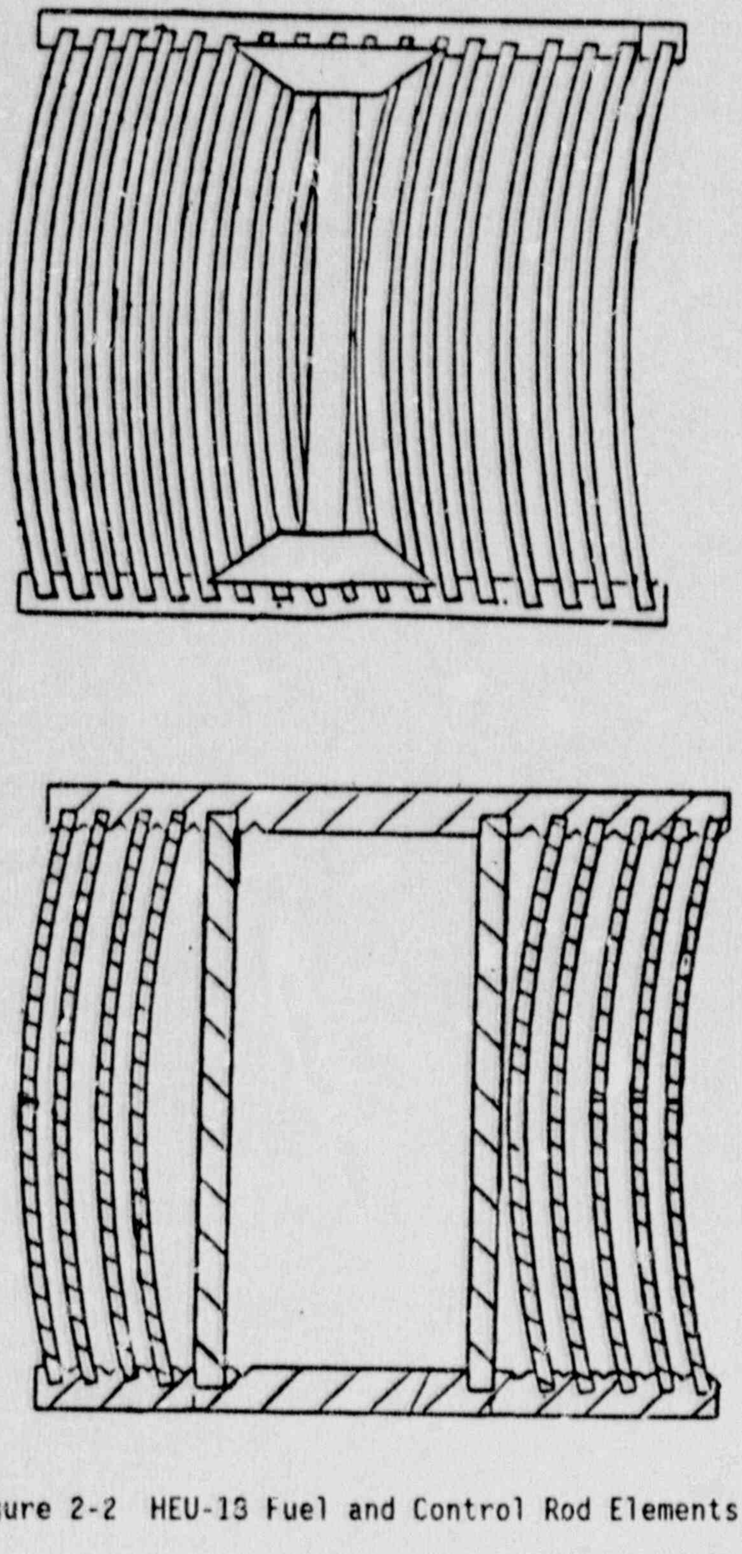

Figure 2-2 HEU-13 Fuel and Control Rod Elements [5].

Important parameters associated with the HEU-18 fuel elements are presented below:

Parameter	Value
1. HEU Fuel Meat	
a. width	0.02 inch
b. length	2.375 inch
c. height	23.5 inch
2. Clad Thickness	0.015 inch
3. Plate Thickness	0.05 inch
4. Water Gap	0.122 inch
5. U-235/plate	10.7 gram
6. U-235/element	192.3 gram

2.4 LEU Fuel

Generic LEU fuel plates have been designed by EG&G Idaho (in cooperation with DOE) and fabricated by Babcock and Wilcox in Lynchburg, Virginia. The plate is made oversized so that it can be "trimmed" to fit different fuel element designs.

Detailed requirements for LEU fuel meat and fuel plates have been published in TRTR specifications [7 - 11]. This information has been reviewed for applicability to the UVAR neutronics work effort [12] and is incorporated in the LEU neutronics analyses presented in this report.

The LEU fuel plate and fuel meat will have dimensions almost identical to the HEU fuel. The LEU fuel meat is 19.75 percent enriched uranium silicide powder (U_3Si_2) dispersed in aluminum powder which is "hot-rolled" to form the fuel core matrix, commonly referred to as the fuel meat. The fuel meat is bonded with, and encased in, an aluminum clad to form the fuel plate.

Specifications for the Generic LEU fuel plate are presented below[13]:

	PARAMETER	VALUE
1.	Type of Fuel	U_3Si_2
2.	Fuel Meat Density	3.47 gram/cm3
3.	U-235 Per Plate	12.5 gram
4.	Plate Thickness	0.050 inch
5.	Plate Width	2.775 inch
6.	Clad Thickness	0.015 inch
7.	Fuel Meat Thickness	0.020 inch
8.	Fuel Meat Width	2.395 inch
9.	Fuel Meat Length	23.25 inch

Generic LEU fuel element designs do not exist because facility-specific elements are generally required. In response to the need for an element design to form a consistent basis for the thermal-hydraulic and neutronics analyses, preliminary UVAR element designs were developed. These designs are presented in references [13] and [14], and have been distributed to LEU Project Principals at both UVA and EG&G Idaho.

The UVAR LEU elements use the generic LEU fuel plate described earlier. The elements will use flat plate fuel and will have the same outer dimensions as previously-used UVAR 12-plate elements. The LEU element designs are based on blueprints for previous HEU elements [15,16]. The element designs currently address only two dimensions. The axial dimension in both the neutronics and thermal-hydraulics analyses is accounted for by an axial dimension function.

Figures 2-3 and 2-4 present the UVAR LEU fuel element and control rod element designs for 22-plate elements (LEU-22) and 18 plate elements (LEU-18). Applicable dimensions for the LEU fuel and control rod elements are presented in the figures.

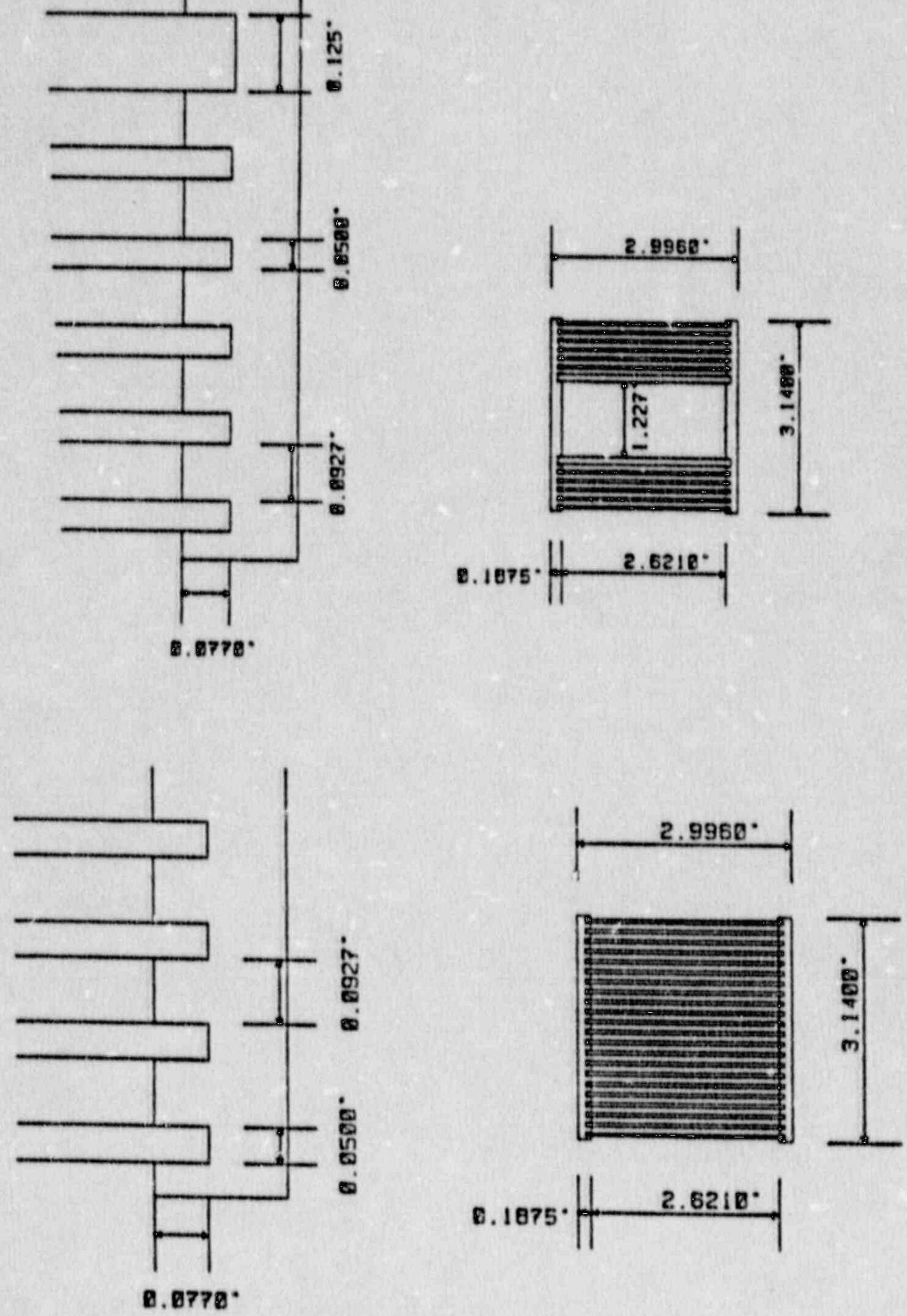

Figure 2-3. LEU-22 UVAR Fuel Element and Control Rod Fuel Element Designs. (Figures by B. Hosticka, April 1988).

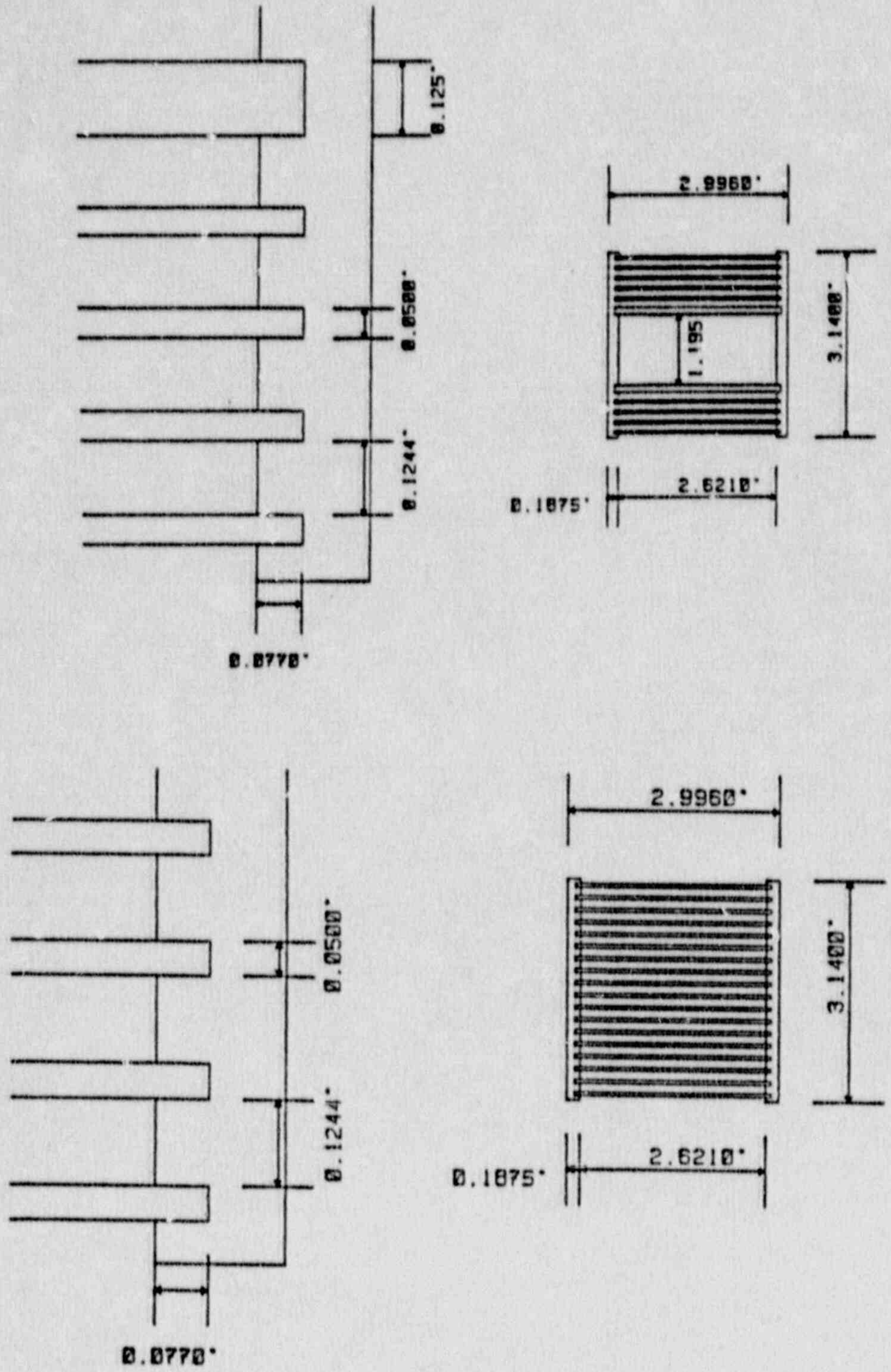

Figure 2-4. LEU-18 UVAR Fuel Element and Control Rod Element Designs (Figures by B. Hosticka, April, 1988).

3.0 METHODOLOGY

Studies presented in this report were performed using several combinations of various main-frame computer codes. The basic methodologies supporting the studies are presented here. Study specific methodologies are presented, as appropriate, in the sections addressing the studies. Computer codes used in the analyses included: 1) LEOPARD; 2)THERMOS; 3) GAMTEC; 4) EXTERMINATOR; and 5) 2DB.

The LEOPARD[17], THERMOS[18], and GAMTEC[19] codes are neutron interaction cross section generator codes and were used to develop energy-dependent cross sections for the analyses. Additionally, the EXTERMINATOR [20] 2-D diffusion theory code was used to help develop control rod cross sections. The methodologies for cross section development are presented in Section 3.1.

2-D diffusion theory codes, 2DB and EXTERMINATOR, were used to develop detailed UVAR core models. The 2DB core model, as modified by the University of Michigan (referred to as 2DB-UM), was used for the bulk of the analyses. The EXTERMINATOR code was used to model the UVAR core for the purposes of calculating delayed neutron fractions and prompt neutron lifetimes. The 2-D diffusion theory codes are described in Section 3.2.

3.1 Methodology For Developing Neutron Cross Sections

Cross sections used in this analysis can be classified as follows:

1. Core-region cross sections
2. Control rod cross sections
3. Reflector cross sections

A different methodology was employed to develop each type of cross section. These methodologies are discussed below.

3.1.1 Core-Region Cross Sections

The LEOPARD computer code was used to develop multi-group cross sections for the UVAR core region. Variations in LEOPARD input parameters were employed to develop temperature and void dependent cross sections used in the temperature and moderator void study presented in Chapter 6. Additionally, the code calculates cross sections associated with fuel depletion at discrete burnup steps.

The LEOPARD code computes two and four group spectrum weighted macroscopic cross sections for an infinitely repeating unit fuel cell in slab geometry. The code allows both lattice and non-lattice portions of the unit fuel cell to be defined. The lattice region is defined as the fuel/clad/moderator repeating array. The non-lattice region contains any materials, such as structure and water spaces, which are not in the lattice. The

UVAR fuel cell model defines the fuel meat, clad, and water gap array of the element to be the lattice region. The non-lattice region contains the element side plates, non-fuel bearing fuel plate edges, control rod guide plates, and control rod water holes. The fuel and control rod elements are slightly smaller than the grid cell dimensions shown in Figure 2-1, thus when loaded in the gridplate, a small amount of water exists between the edges of adjacent elements in all directions. This water is considered non-lattice.

The LEOPARD models "distort" the actual fuel and control rod element dimensions somewhat while conserving materials and surface area. The distortion consists of "compressing" the cell in the y direction and correspondingly "stretching" the cell in the x direction. This distortion was performed so that the lattice region of the cell extends completely across the grid cell in the x direction, thus eliminating the small amount of water that actually lies between each element in the x direction. This distortion technique, developed by Fehr [2], allows for an uninterrupted fuel lattice region when several elements are loaded together in the 2-D core models.

Burn-up cross sections account for fuel depletion, xenon and samarium buildup, and other fission products.

Two and four group cross sections calculated for the fuel lattice, non-lattice and control rod non-lattice regions are presented in Appendix A.

3.1.2 Control Rod Cross Sections

Two group control rod cross sections were developed using a combination of various features provided in the THERMOS, GAMTEC, and EXTERMINATOR codes. The method of developing control rod cross sections is quite involved and time consuming to perform. Several different modeling techniques were investigated by Wasserman [22]. The Wasserman study yielded methodologies for control rod modeling that produced results consistent with experimental data. The Wasserman study specifically addressed control rods in the UVAR HEU-18 fueled core. An analogous methodology was developed to calculate control rod cross sections for the LEU fuel. Control rod cross sections were used to calculate control rod worths (Section 4). A brief description of the methodology is presented here; however, the reader is referred to Wasserman (and Reference [3]) for a detailed presentation.

Control rods are difficult to model using diffusion theory computer codes because the control rod is a strong absorber and creates a steep local flux gradient. Diffusion theory cannot adequately handle the steep gradient, thus transport theory is required. The methodology developed to model the control rod region consists of calculating cross sections for that region which, when used in a full 2-D diffusion core model, produce the correct results. These cross sections are called "effective" diffusion theory cross sections because they help the diffusion theory code "effectively" handle the local rod transport problem.

The effective cross sections were developed by first calculating transport thermal microscopic cross sections for the control rod region. A 1-D THERMOS slab transport model of a control rod fuel element with control rod material in the central region was developed. The THERMOS model calculated region-smeared microscopic cross sections and region-dependent neutron absorption fractions.

Fast group microscopic cross sections were developed with a cylindrical GAMTEC model control rod fuel element. GAMTEC calculates fast group cross sections using a P-1 approximation. GAMTEC also calculates resonance absorption fractions for the cell model.

The thermal and fast microscopic cross sections were input into a 2-D EXTERMINATOR model of a rodded control rod element using x-y geometry. The area of the control rod region in the EXTERMINATOR model corresponds to the area used for the control rod water hole region of the 2DB models.

The thermal absorption cross sections were manually adjusted in the EXTERMINATOR model until the thermal absorption fractions in the fuel and control rod regions matched those predicted by the THERMOS model. The fast absorption cross sections in the EXTERMINATOR model were also manually adjusted such that the fraction of neutrons reaching thermal energies matched the resonance escape probability predicted by the GAMTEC P-1 approximation.

The methodology described above was applied to each fuel type (i.e., HEU-18, LEU-18, LEU-22). Resulting macroscopic cross sections are presented in Appendix A.

3.1.3 Reflector Cross Sections

Graphite and water are the predominant reflector materials for the UVAR reactor. Other reflector materials are addressed in Section 7.

Two and four group water and graphite reflector cross sections were provided by Argonne National Laboratory (ANL) EPRI-CELL computer models. These cross sections are presented in Appendix A.

Two group graphite reflector cross sections were developed by Wasserman at UVA using the GAMTEC code. The UVA cross sections were used in the 2DB core models and are presented in Appendix A. The UVA graphite cross sections were found to be consistent with the ANL cross sections.

3.2 Diffusion Theory Modeling Of The UVAR Core

The 2DB code was used to model the UVAR core for the purposes of calculating the k-effective eigenvalue solutions. Studies presented in this report focus on reactivity effects associated with various core changes as determined from changes in the 2DB calculated k-effective. The EXTERMINATOR code was used to develop

2-D UVAR core models for the purpose of calculating delayed neutron fractions and prompt neutron lifetimes. The EXTERMINATOR model is analogous to the 2DB model and is addressed in Section 8.

Fehr [2] developed the basic 2DB core model for HEU-18 and for LEU fuels. The Fehr models were revised and updated somewhat to be consistent with the UVA LEU element designs described in Section 2. The reader is referred to Fehr for detailed modeling descriptions.

The 2DB core model consists of a 60-by-62 mesh in x-y geometry. The model extends about 10 to 15 cm beyond the UVAR grid plate in both directions. The outer boundaries were defined with a zero flux condition. The axial direction is accounted for by spatially-dependent axial buckling terms developed from ANL 3-D UVAR core models.

Cross sections described in Section 3.1 were used as input into the code. LEOPARD-developed cross sections were input directly through the LINX computer code while other cross sections were input by hand.

Two basic core models were considered in this analysis; the 4-by-4 and 4-by-5 core model. The 4-by-4 core model, presented in Figure 3-1, consists of 12 fuel and 4 control rod elements in a 4-by-4 array. Figure 3-2 presents the 4-by-5 core model which consists of 16 fuel elements and 4 control rod elements in an 4-by-5 array. Individual fuel elements are identified by the number appearing in the lower left hand corner of the fuel element cells shown in Figures 3-1 and 3-2. The cores are shown with an optional full graphite reflector, which means that each grid plate location surrounding the core is loaded with a graphite element.

Core models shown in Figures 3-1 and 3-2 use "staggered" control rod locations. Staggered control rod locations are necessary because the emergency core cooling system sprays from the east and west directions. If the control rod locations were not staggered, spray water to adjacent elements would be impeded.

The models are built with unit cells, each with dimensions corresponding to the grid cells described in Section 3.1.

The core model was "built" by placing appropriate material cross sections in desired model cells. Fuel region cross sections developed with the LEOPARD code were input in cells to simulate fuel elements. LEOPARD control rod element cross sections were input into cells to simulate control rod elements. Control rod cross sections and reflector cross sections were utilized in the same manner.

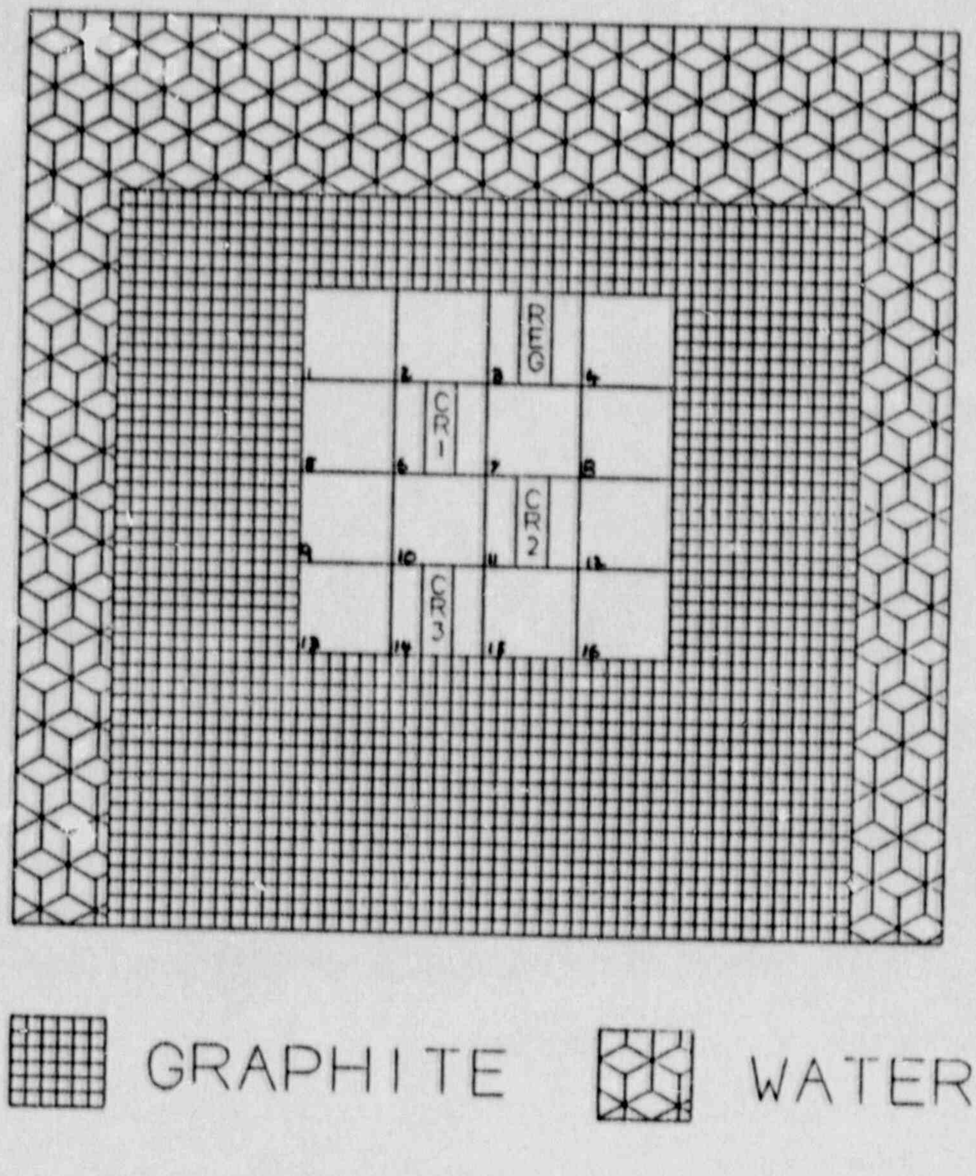

Figure 3-1. UVAR 4-by-4 Core Model. (Figure by M. Fehr, January, 1989)

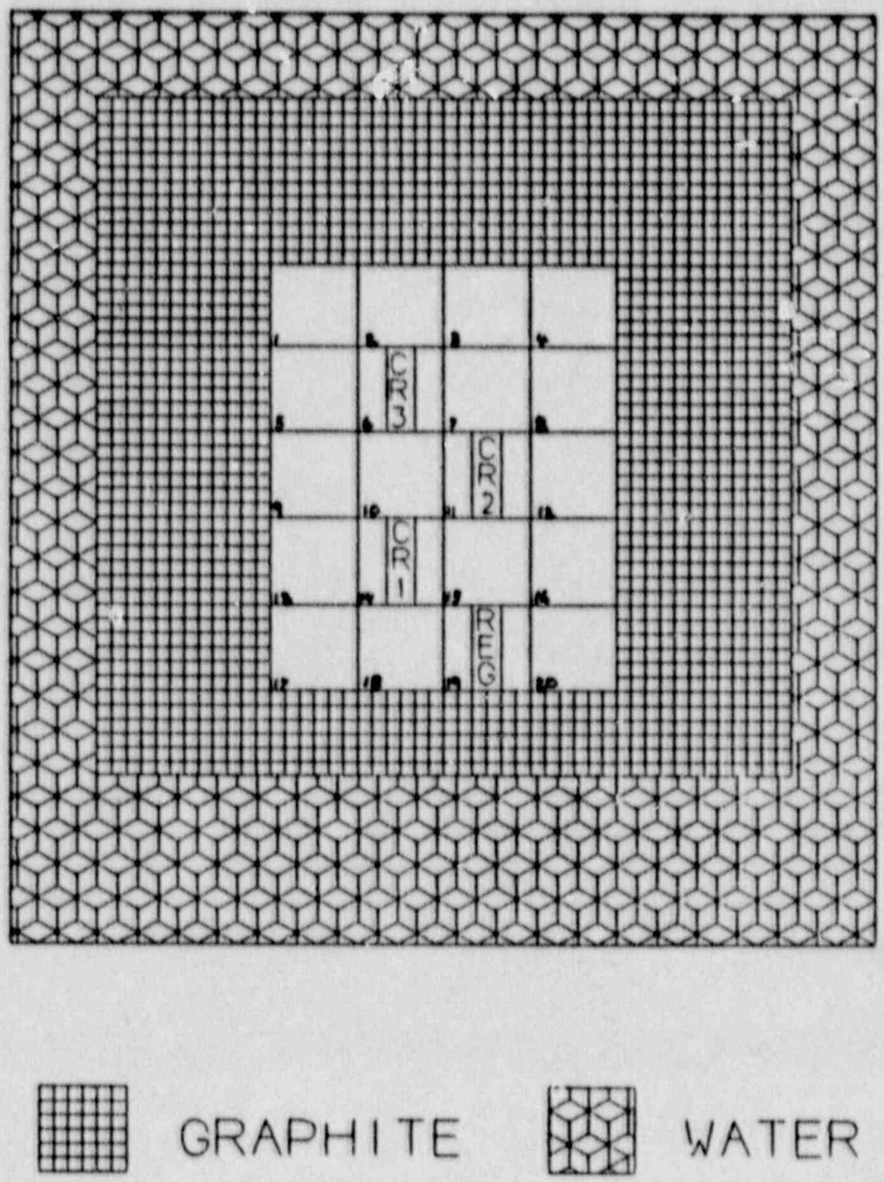

Figure 3-2. UVAR 4-by-5 Core Model. (Figure by M. Fehr, January, 1989)

CHAPTER 4.0 CONTROL ROD WORTH STUDY

Control rod worths have been determined for 4-by-4 and 4-by-5 UVAR cores constructed with the LEU-22, LEU-18, and HEU-18 fuel options. The term "control rod" encompasses both the safety rods (Rods 1, 2, and 3) and the regulating rod as described in Section 2. The effects of core life and core reflector material on control rod worth have also been determined. Additionally, control rod worth as a function of the positioning of the rods in the core has been investigated.

4.1 Rod Worths In 4-by-4 and 4-by-5 UVAR Cores

Control rod worths have been determined for both the 4-by-4 and 4-by-5 graphite reflected UVAR core models for each fuel option. Rod worths were determined by replacing control rod water hole cross sections by the control rod cross sections presented in Appendix A. Control rod locations are shown in Figures 3-1 and 3-2 (See Chapter 3) for the 4-by-4 and 4-by-5 cores, respectively. Control rod worths were initially developed in the Spring of 1988 and were documented in a UVA internal memorandum [23]. The neutronics models have since been revised and the rod study has consequently been updated. Results of the updated study, not significantly different from the original study, are presented here.

Table 4.1 presents calculated control rod worths for the UVAR 4-by-4 and 4-by-5 cores for each fuel option. Rod worths presented in Table 4.1 have an estimated computational error of the order of five percent.

Table 4.1 Control Rod Worths For the UVAR 4-by-4 and 4-by-5 Cores.

Rod Inserted	- Rod Worths (%$\Delta\rho$) - LEU-22	LEU-18	HEU-18
I. 4-by-4 UVAR Core			
a) Reg. Rod	0.67	0.66	0.58
b) Rod 1	3.75	3.69	3.77
c) Rod 2	3.93	3.89	3.97
d) Rod 3	2.32	2.23	2.25
II. 4-by-5 UVAR Core			
a) Reg. Rod	0.39	0.39	0.33
b) Rod 1	2.46	2.38	2.47
c) Rod 2	3.21	3.18	3.21
d) Rod 3	2.79	2.75	2.79

Information provided in Table 4.1 shows that rod worths are not significantly affected by the different fuel types.

The maximum control rod worth is that of Safety Rod 2. This is expected because Rod 2 is the most centrally located rod and is consequently exposed to higher flux and carries a higher adjoint importance than the other rods. This is also consistent with the fact the peak flux value (determined in Section 5) is also found in the same region.

Experimentally determined control rod worths for the 4-by-4 HEU-18 core are available [24] and are compared with the calculated worths in Table 4.2. Experimentally determined worths were converted from dollars to % $\Delta\rho$ using an effective delayed neutron fraction of 0.0074. (Information presented in Chapter 8 shows that an effective delayed neutron fraction of 0.0074 is appropriate for the HEU core.)

Table 4.2 Comparison of Experimentally Determined and Calculated Rod Worths for the 4-by-4 HEU-18 UVAR Core.

Rod ID	Experimentally Determined Worth (%$\Delta\rho$)	Calculated Worth (%$\Delta\rho$)	Difference
Reg. Rod	0.43	0.58	35%
Rod 1	3.52	3.77	7%
Rod 2	3.70	3.97	7%
Rod 3	2.27	2.25	<1%

The calculated control rod worths presented in Table 4.2 match well with the experimental values. It should be noted that an estimated 10 percent absolute error is considered appropriate for the experimental values. The calculated worth of the regulating rod is a bit high; however, because of the minor role that the regulating rod plays in core safety (the regulating rod is non-scramable), no further calculational refinement was considered necessary. (ANL has privately stated [25] that they also over-calculate the worth of the regulating rod. The reason for this is not readily apparent, but may indicated a need to examine the cell boundary conditions or the cross section library for iron and other stainless steel constituents.)

4.2 Core-Life Effects On Control Rod Worth

Core-life effects on control rod worth were determined for the single case of a 4-by-5 graphite reflected core using LEU-22 fuel. The results of this study are generally applicable to other control rods and fuel options.

The worth of control rod 1 was determined at four different stages of core burnup: 1) 0 MW-days; 2) 4 MW-days; 3) 194 MW-days; and 4) 394 MW-days. The control rod worths calculated at each stage of core burnup are presented in Table 4.3.

Table 4.3 Core-Life Effects on Control Rod Worth

Core Burnup (MW-day)	Worth (%$\Delta\rho$)
0	2.46
4	2.51
194	2.57
394	2.62

The results above show that control rod worth tends to increase slightly over core life. The worth associated with 0 MW-day burnup is calculated for a "clean" xenon-free core. Experiments have shown that the UVAR reaches equilibrium xenon conditions after about 40 hours of continuous 2 Megawatt operation (i.e., 80 MW-hrs). This corresponds roughly to the first burnup step of 4 MW-days (96 MW-hrs). The difference in rod worth between the 0 MW-day and 4 MW-day cases is most likely a result of changes in spatial flux shape due to xenon rather than as a result of fuel burnup. Control rod worth changes for the longer time steps (all at equilibrium xenon conditions) are due to fuel burnup.

Because control rod worths tend to increase with core burnup (and with xenon buildup), the shutdown (safety) margin also increases in the direction of conservatism - a favorable trait. Control rod worth curves form the basis for demonstrating compliance with NRC requirements and determining the worth of experiments. Because control rod worths change with core burnup, the rods should be periodically recalibrated to account for the burnup effect. Currently, UVAR procedures require rod recalibration every 1200 Mw-hours (50 Mw-days) for just this reason. As discussed earlier, control rod worths may change due to xenon buildup over operations extending over several days; however, no method exists to account for this change. Because rod worths swing in the conservative direction (i.e., greater shutdown margins) this effect is not deleterious to safe operation.

4.3 Reflector Effects On Control Rod Worths

Reflector effects on control rod worth were determined for three representative reflector options for the LEU-22 4-by-5 UVAR core. The reactivity worth of control rod 1 was determined for the UVAR using Reflector Options 1, 5, and 13 as described in Section 7.1.

Reflector Option 1 consists of a full grid plate of graphite surrounding the centrally-located 4-by-5 core. Reflector Option 5 is similar to Option 1 except that the entire East core face is reflected by water. Reflector Option 13 consists of a full water reflector surrounding the 4-by-5 core.

The reactivity worths of control rod 1, calculated for the UVAR core using the various reflector options are presented in Table 4.4. Control rod worths were calculated relative to the unrodded core.

Table 4.4 Reflector Effects on Control Rod Worth

Reflector Option	Control Rod 1 Worth (%$\Delta\rho$)
1	2.47
5	2.75
13	2.84

The results presented above show that control rod worth tends to increase as the core graphite reflector is replaced by water reflector. The rod worth for the all-water reflector (Option 13) is about 15 percent higher than for the all-graphite reflector (Option 1). This implies that control rod worths should be reexamined (recalibrated) following significant changes in core reflector. UVAR procedures address this effect by requiring control rod recalibration with removal or insertion of one or more graphite elements next to the core.

4.4 Control Rod Position Effects

Control rod worths for control rods in the alternate locations shown in Figure 4-1 have been calculated for LEU-22 fuel.

It has been suggested that rotating the UVAR core by 45 degrees would lead to higher neutron fluxes in certain experimental facilities. As discussed in Chapter 3, the UVAR core models used staggered rod positions to prevent interfering with the emergency core cooling system (ECCS). If the core is rotated the rod pattern shown in Figure 4-1 is proposed to prevent interference with the ECCS.

Reactivity worths of the control rods in the alternate positions shown in Figure 4-1 for LEU-22 fuel are presented in Table 4.5

Table 4.5. Control Rod Worths For Alternate Rod Locations In UVAR 4-by-5 Core.

Rod Inserted	Rod Worth (% $\Delta\rho$)
Reg Rod	0.80
Rod 1	2.56
Rod 2	2.74
Rod 3	2.70

Information provided in Table 4.5 shows that the safety rod worths (Rods 1,2, and 3) show little variation, as expected, due to the symmetrical nature of their locations.

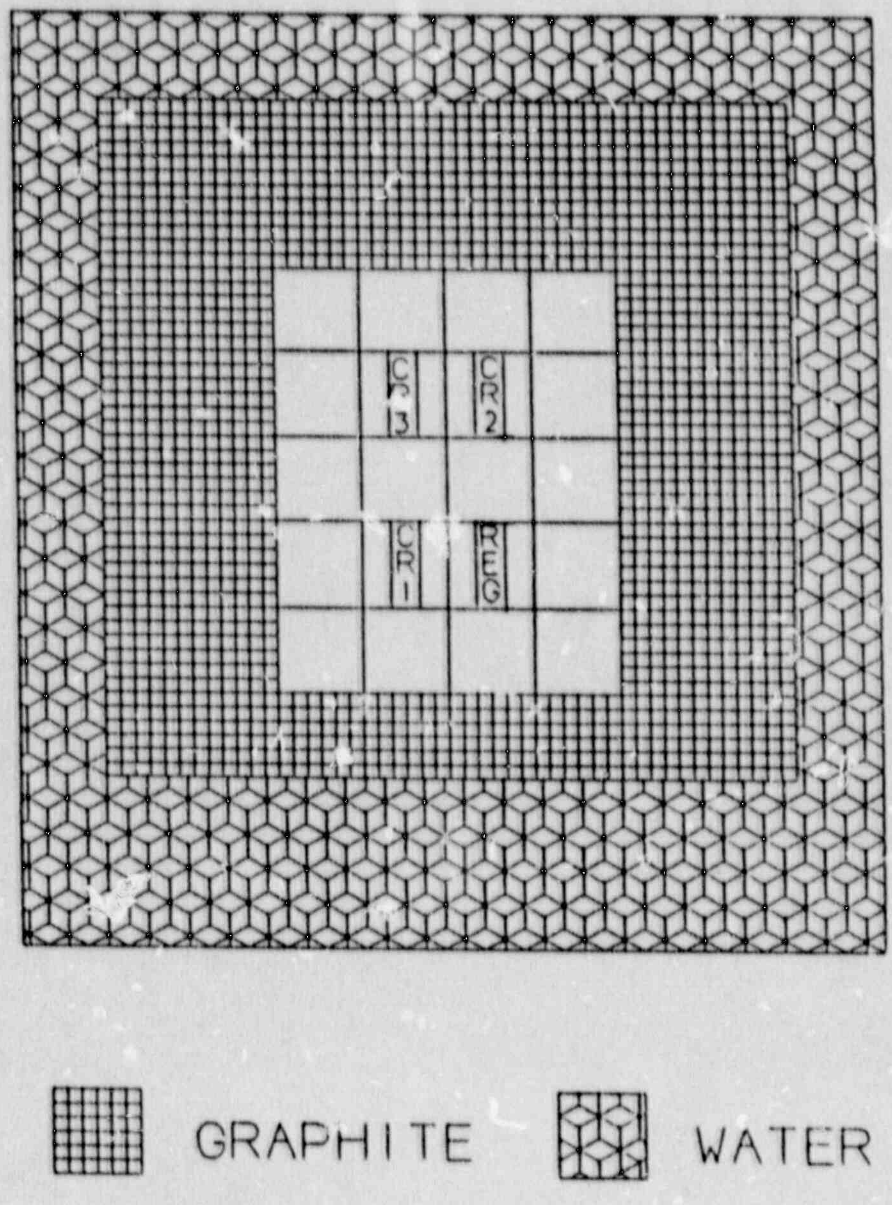

Figure 4-1. Alternate Control Rod Locations for UVAR 4-by-5 Core.

Rod worths for Rods 1 and 3 in the alternate locations are about the same as calculated in the staggered-rod positions (Table 4.1) because their relative core locations are similar. Rod 2 in the alternate-location model has about 1/2% $\Delta\rho$ less worth than in the staggered-location model. This is because Rod 2 is more centrally located in the staggered model resulting in higher importance. By the same argument, the regulating rod worth in the alternate model is more than twice that calculated in the staggered model.

The sum of all control rod worths in the alternate model is about the same as for the staggered model.

4.5 Control Rod Worth Study Summary

Based on the results presented above, the following summary statements can be made:

1. Control rod worths are not significantly affected by the choice of fuel option.
2. Control rod worths are dependent on the rod position in the core with centrally-located rods having the highest worths.
3. Good agreement was found between experimentally determined and calculated rod worths.

4. Control rod worths change with xenon build-up and core burn-up implying that control rods should be periodically recalibrated.
5. Control rod worths change with core reflector changes implying the need to recalibrate rods following core reflector changes.
6. Control rod worths vary for the alternate-rod-position model considered; however, the sum of the rod worths was almost identical to that calculated for the staggered-rod-position model.

5.0 RADIAL PEAKING FACTORS

Radial peaking factors have been determined for the UVAR core for the purpose of supporting the Thermal Hydraulics Analysis portion of the HEU to LEU Conversion effort. The sensitivity of radial peaking factors to variations in core configuration, control rod element orientation, control rod insertion, core burnup, and core reflector options have been evaluated. Axial peaking factors are not addressed in this analysis; however, experimental data pertaining to axial peaking factors for the HEU UVAR are available [26].

Peaking factors were determined using the 2DB computer code described in Section 3. The 2DB code provides a mesh-centered flux map (and optional edge-centered fluxes) for each energy group. The 2DB code also provides average group flux values for specified edit regions. The "active" or "lattice" fuel region of the reactor core, where heat production occurs, was defined as a single edit region. Peaking factors were calculated by taking the peak-to-average thermal flux ratio found in the active fuel region of the reactor core.

Thermal flux peaking factors are considered representative of power peaking factors. Neglecting fast fission effects, power production can be considered proportional to $\Sigma_f \phi_{th}$, where Σ_f is the thermal macroscopic fission cross section and ϕ_{th} is the thermal neutron flux. If Σ_f is considered constant, power production is proportional to ϕ_{th}. For all beginning-of-life (BOL) unburned UVAR core models, Σ_f was indeed constant over the fuel region. All analyses presented below use a BOL core model except for the core burnup analysis presented in Section 5.5. (The core burnup analysis accounts for a non-uniform Σ_f distribution.)

Thermal flux peaking factors were used in the original HEU UVAR thermal-hydraulic safety analysis and in the UVAR 2 megawatt upgrade safety analysis, and are considered appropriate for use in the LEU thermal-hydraulic analysis. The thermal-hydraulic analysis focuses on a single "hot-channel" and relies on peaking factors to relate the hot channel to the nominal channel which is normalized to core size and average power.

The calculated peak thermal flux in the fuel region was found to occur immediately adjacent to a control rod element water hole. The model mesh boundary between the water hole and fuel region is located between the control rod guide plate and the first adjacent fuel plate (see Figures 2-3 and 2-4). Consequently, the flux at the mesh-edge boundary between the fuel region and water hole is higher than the flux at the center of the first fuel region mesh. Although the mesh edge flux is higher, the channel between the first adjacent fuel plate and the control rod guide plate is not considered the "hot-channel" because it only receives heat from the single fuel plate. The next adjacent channel is the "hot-channel", receiving the maximum heat flux from the two surrounding fuel plates. Mesh-centered flux values for the computer models are located in the "hot-channel" and are therefore considered more appropriate than edge-centered values. Mesh-centered fluxes have been used throughout this analysis.

The LEU peaking factor analysis focused on the four areas of study described below:

1) 4-by-4 and 4-by-5 graphite reflected core;

2) control rod element rotation effects;

3) control rod insertion effects;

4) core burnup effects; and

5) core reflector effects.

The results of these studies are presented below.

5.1 Radial Peaking Factors for 4-by-4 and 4-by-5 UVAR Cores

Radial peaking factors have been determined for the UVAR reactor in 4-by-4 and 4-by-5 graphite-reflected, unrodded BOL core configurations. Peaking factors for LEU-22, LEU-18, and HEU-18 fuel options have been evaluated for each core configuration.

Radial peaking factors determined for the above-defined core configurations and fuel options are presented in Table 5.1.

Information presented in Table 5.1 shows that peaking factors are slightly higher in LEU fuel than in HEU fuel. This is primarily due to a harder flux spectrum downscattering in the control rod water holes. The LEU-18 peaking factors are about 4 to 6 percent higher than the HEU-18 peaking factor.

Table 5.1. Radial Peaking Factors for UVAR 4-by-4 And 4-by-5 Core Configurations With Various Fuel Options.

Core Configuration/Fuel Option	Radial Peaking Factor
1. 4-by-4 Core Configuration	
a) LEU-22	1.72
b) LEU-18	1.67
c) HEU-18	1.61
2. 4-by-5 Core Configuration	
a) LEU-22	1.81
b) LEU-18	1.76
c) HEU-18	1.66

Peaking factors increase with core size and with the number of plates per fuel element. Peaking factors for the 4-by-5 cores are about 3 to 5 percent higher than for the 4-by-4 cores. The peaking factor for LEU-22 fuel is also about 3 percent higher than for LEU-18 fuel.

Peak thermal flux values were found in locations immediately to the left of the Control Rod 2 water hole (see Figures 2.3 and 2.4). This location is consistent with the measured peak flux found by Sternberg [26].

Limited experimental data is available on UVAR HEU radial peaking factors. A radial peaking factor of 1.37 was experimentally determined for a partially-burned UVAR 4-by-4 HEU-12 (12 flat plates per element) core via foil flux mapping [5]. An estimated experimental error of 10 percent is considered appropriate for this value.

This experimental value was subsequently "corrected" [5] using a 1-D neutronics code to predict a value of 1.45 for the HEU-18 core. The value of 1.45 is about 10 percent lower than the value of 1.61 estimated in this analysis, which appears to be within the experimental and computational uncertainty.

The 4-by-4 core configurations are the limiting core configurations (for each fuel type) for the Thermal Hydraulic Analysis [4]. This is primarily due to the higher average power density and non-element bypass flow rate associated with the small cores. These factors outweigh the importance of the slight increase in peaking factors associated with the larger cores. No core larger than 4-by-5 was considered in this analysis.

5.2 Control Rod Element Rotation Effects on Radial Peaking Factors

The control rod elements are asymmetrical in that there is one more fuel plate on one side of the control rod hole than on the other side (see Section 2). Because the LEU fuel elements will use flat plate fuel, it should be possible to load the control rod elements (and fuel elements) into the grid plate in two different orientations, each 180 degrees rotated from the other.

The curved plate HEU-18 fuel, currently used in the UVAR, cannot be rotated. This is due to the physical nature of the HEU-18 curved plate elements which interlock and consequently must all be loaded in the same orientation.

Radial peaking factors presented in Section 5.1 were calculated for cores in which all control rod elements were loaded with the extra plate on the left side of the element. To characterize the effect of different control rod orientations on peaking factors, three different control rod orientation scenarios were analyzed:

Scenario 1. All control rods loaded with the extra plate on the right side of the element.

Scenario 2. Rods 1 and 3 loaded with the extra plate on the right side of the element; Reg Rod and Rod 2 loaded with the extra plate on the left side of the element.

Scenario 3. All control rods loaded with the extra plate on the left side of the element.

Control rod locations are shown in Figures 3-1 and 3-2.

Table 5.2 presents radial peaking factors determined for the different control rod element orientation scenarios. It should be noted that values presented for the HEU-18 fuel option in Scenario

2 are fictitious because the curved plate fuel cannot be physically loaded in opposing orientations. HEU-18 peaking factors for Scenario 2 are presented for comparison purposes only.

Table 5.2 Radial Peaking Factors For Control Rod Orientation Scenarios

Core Configuration/ Fuel Loading	Radial Peaking Factors		
1) 4-by-4 Core Configuration	Scenario 1	Scenario 2	Scenario 3*
a) LEU-22	1.72	1.66	1.72
b) LEU-18	1.67	1.62	1.67
c) HEU-18	1.61	1.57	1.61
2) 4-by-5 Core Configuration			
a) LEU-22	1.81	1.75	-
b) LEU-18	1.76	1.70	-
c) HEU-18	1.66	1.62	-

* Peaking factors for Scenario 3 were calculated for the 4-by-4 core configuration only.

Information presented in Table 5.2 shows that radial peaking factors for Scenario 2 are about 2.4 to 3.5 percent lower than those presented in Scenario 1. Scenario 3 values are virtually identical to Scenario 1 values. This is reasonable because of the near symmetry of the core and the fact that all elements have the same orientation in Scenarios 1 and 3.

The differences in values can be taken as an estimate of the overall precision associated with calculated peaking factors.

5.3 Control Rod Insertion Effects on Radial Peaking Factors

The peaking factors presented in Sections 5.1 and 5.2 were calculated for unrodded cores. In order to gain insight into the effect of control rod insertion on peaking factors, the LEU-22 4-by-4 graphite reflected BOL core was analyzed with various control rod insertion scenarios. This analysis is not completely rigorous due to the limitations on diffusion theory when handling interfaces at control rod boundaries and the approximations involved in developing cross sections for the control rod regions (see Section 4). None the less, this analysis provides insight into the general behavior of peaking factors with control rod insertion.

Table 5.3 presents the radial peaking factors associated with the LEU-22 4-by-4 BOL graphite reflected core with various control rod insertions.

Information provided in Table 5.3 shows that radial peaking factors increase by as much as 3 percent with single rod insertions except for Rod 2. Because the peak flux location of the unrodded core is adjacent to Control Rod 2, insertion of rods other than Rod 2 push the flux up in the Rod 2 region causing an increased peak. Similarly, insertion of Rod 2 depresses the flux in that region and "pushes" the peak location towards the Rod 1 water hole. Consequently, the flux shape is flattened and the peaking factor decreases by about 2 percent.

Table 5.3. Radial Peaking Factors for LEU-22 4-by-4 Graphite Reflected Core With Various Rod Insertions.

Core Status	Peaking Factor	Peak Location
1. Unrodded Core (No rods inserted)	1.72	Adjacent left side of Rod 2
2. Rod 1 Inserted Only	1.77	Adjacent left side of Rod 2
3. Rod 2 Inserted Only	1.69	Adjacent Right Side of Rod 1
4. Rod 3 Inserted Only	1.75	Adjacent Left side of Rod 2
5. Reg Rod Inserted Only	1.76	Adjacent Left side of Rod 2

The Peaking Factors presented in Table 5.3 vary from 1.69 to 1.77 (about 5%) depending on which rod is inserted. Combinations of more than one rod inserted at a time were not evaluated because the UVAR cannot be taken critical with more than one rod fully inserted due to regulatory restrictions on shutdown margin and excess reactivity.

5.4 Core-Life Effects on Radial Peaking Factors

The peaking factors presented in Sections 5.1, 5.2, and 5.3 were calculated for beginning of life (BOL), unburned cores. During reactor operation, the core is slowly "burned" resulting in less U-235 and a buildup of fission products and poisons. The effect of core burnup on peaking factors was determined by analyzing a 4-by-5 LEU-22 graphite-reflected core at various burnup times. Burnup times evaluated were: 1) no burnup; 2) 194 MW-days burnup; and 3) 394 MW-days burnup.

As discussed earlier, the validity of the thermal flux peaking factor is tied to the assumption that Σ_f remains constant over the fuel region. This assumption is valid for BOL cores; however, because cores burn unevenly, Σ_f is not constant throughout the fuel region in a burned core. In order to account for the non-uniform Σ_f distribution in the core, the following approximation scheme was used to calculate peaking factors for burned cores:

1. The peak value of $(\Sigma_f \phi_{th})_{local}$ was determined by multiplying the local Σ_f determined for each fuel element by the associated mesh thermal fluxes. In each case the location of the peak value of $(\Sigma_f \phi_{th})_{local}$ coincided with the location of the peak thermal flux.
2. An average value $\bar{\Sigma}_f$ was determined by simply summing element specific Σ_f's over the 20 elements and then dividing by the 20 elements. The average thermal flux ($\bar{\phi}_{th}$) in the active fuel region was provided as output by the 2DB code.
3. The peaking factor was then estimated as follows:

$$\text{peaking factor} = \frac{(\Sigma_f \phi_{th})_{local\ peak}}{\bar{\Sigma}_f\ \bar{\phi}_{th}}$$

Ideally, the denominator would be a flux-weighted average of Σ_f over each fuel region mesh point. Unfortunately, this value is not readily available from the information provided in the 2DB output*. The above described weighting scheme provides an adequate approximation for determining the general behavior of peaking factors with core burnup.

Table 5.4 presents radial peaking factors for the UVAR 4-by-5 LEU-22 graphite reflected core with 0, 194, and 394 Mw-days burnup. Also presented in Table 5.4 is the min-to-max variation in Σ_f over the core region for each burnup step.

Table 5.4. Core Life Effects on Radial Peaking Factors for the LEU-22 4-by-5 Graphite Reflected Core.

Burnup (MW-day)	Peaking Factor	Σ_f variation
0	1.81	0%
194	1.77	3%
394	1.73	6%

*Certain edits were added to the 2DB code by the University of Michigan that appear to address power peaking factors; however, there are unresolved inconsistencies in these edits. Preference was given to the original code edits for flux values which were used throughout the peaking factor analysis.

Information presented in Table 5.4 shows that peaking factors decrease with core life. This is consistent with the fact that there is more local burnup in the peak flux region than in the rest of the core resulting in a flattened flux distribution.

5.5 Core-Reflector Effects on Radial Peaking Factors

Reflector options for the UVAR core were analyzed for the LEU-22 and LEU-18 fuel options as discussed in Chapter 7. Peaking factors associated with the various reflector options have been determined. Table 5.5 presents peaking factors associated with three representative reflector options for LEU-22 and LEU-18 fuel.

Table 5.5. Core-Reflector Effects on Radial Peaking Factors

	--- $\Delta\rho$(%Δk/k) ---	
Reflector Option	LEU-22	LEU-18
1. All-Graphite Reflector	1.73	1.67
2. Single Row of Graphite Surrounding Core	1.75	1.69
3. All-Water Reflector	1.76	1.73

Peaking factors were found to be relatively insensitive to the various reflector options and showed a maximum variability of about 3 percent.

5.6 Radial Peaking Factor Summary

Peaking factors for various core configurations, control rod orientations, rod insertions, core burnup, and reflector options have been obtained. Based on information presented above, the following conclusions have been made:

1. Radial peaking factors for LEU fuel are slightly higher than for HEU fuel. Peaking factors increase with core size and with the number of fuel plates per element.
2. Radial peaking factors may vary by as much as 3.5 percent depending on control rod orientations.
3. Insertion of a single control rod can produce a change in peaking factor ranging from a 2 percent decrease to a 3 percent increase.
4. Peaking factors decrease somewhat with core life due to the higher burnup occurring in the peak flux region.
5. Peaking factors are relatively insensitive to the core-reflector option, showing a maximum variability of about 3 percent.

CHAPTER 6.0 TEMPERATURE AND MODERATOR EFFECTS STUDY

Temperature and moderator void effects have been characterized for the UVAR reactor. Section 6.1 addresses temperature effects and Section 6.2 addresses moderator void effects.

6.1 Temperature Effects

Temperature effects have been determined for the UVAR reactor for both a 4-by-4 and 4-by-5 graphite reflected core configuration. Temperature effects on core reactivity have been quantified separately in terms of: 1) doppler effect; 2) moderator temperature effect; 3) power defects; and 4) gross system heating effect. Temperature effects for the 4-by-4 core configuration were determined in the Spring of 1988 and were documented via a UVA internal memorandum [27]. The temperature-effects analysis for the 4-by-5 core configuration was performed in early 1989 and incorporates the latest revised core models.

Temperature effects presented in the following sections are determined from the change in core reactivity associated with that effect relative to the reactivity associated with a "reference" core condition. Reference core conditions were determined from a review of information used in the UVAR HEU-to-LEU thermal hydraulics work, where the fuel-plate-to-moderator-temperature differential was determined to be about 9°C for 22 plate elements and about 12°C for 18 plate elements. The temperature gradient across the thin fuel plate was assumed to be negligible.

Temperatures used for the reference cores are provided below:

Element Type	Fuel Plate Temperature (°C)	Moderator Temperature (°C)
22 plate	30	21
18 plate	33	21

Temperature effects for the 4-by-4 cores were determined for LEU-22, LEU-18, and HEU-18 fuel options. Temperature effects for the 4-by-5 cores were determined for LEU-22 and HEU-18 fuel options only.

6.1.1 Doppler Effects

Doppler effects for the UVAR core were determined by adjusting the resonance temperature parameter in the LEOPARD code. Table 6.1 presents reactivity worths and doppler coefficients associated with resonance temperatures of 75, 100, and 200 degrees celsius. Differential reactivity worths were determined from the change in k-effective associated with each resonance temperature relative to the reference case k-effective. Doppler coefficients were determined by dividing reactivity worths by the associated change in resonance temperature.

Doppler coefficients for each fuel option remain relatively stable over the 75°C to 200°C temperature range. Doppler coefficients for LEU are about an order of magnitude greater than

Table 6.1. Doppler Effects for the UVAR Reactor

Resonance Temperature (°C)	Reactivity Worth $\Delta\rho$	Doppler Coeff ($\Delta\rho$ per °C)
I. UVAR 4-by-4 Core Configuration (1988 Study)		
	LEU-22 FUEL	
75	-5.3×10^{-4}	-1.2×10^{-5}
100	-8.1×10^{-4}	-1.2×10^{-5}
200	-1.9×10^{-3}	-1.1×10^{-5}
	LEU-18 FUEL	
75	-4.3×10^{-4}	-1.0×10^{-5}
100	-6.7×10^{-4}	-1.0×10^{-5}
200	-1.6×10^{-3}	-9.5×10^{-6}
	HEU-18 FUEL	
75	-3.8×10^{-5}	-9.0×10^{-7}
100	-5.9×10^{-5}	-8.8×10^{-7}
200	-1.4×10^{-4}	-8.3×10^{-7}
II. UVAR 4-by-5 Core Configuration (1989 Study)		
	LEU-22 FUEL	
75	-5.1×10^{-4}	-1.1×10^{-5}
100	-8.4×10^{-4}	-1.2×10^{-5}
200	-1.8×10^{-3}	-1.1×10^{-5}
	HEU-18 FUEL	
75	-5.6×10^{-5}	-1.3×10^{-6}
100	-8.8×10^{-5}	-1.3×10^{-6}
200	-2.1×10^{-4}	-1.2×10^{-6}

for HEU fuel. This is consistent with the fact that LEU fuel has a much higher uranium-238 loading and is thus more sensitive to resonance effects. Similarly, LEU-22 fuel has a slightly higher doppler coefficient than LEU-18 because of the higher U-238 loading per element. It should be noted that the values presented in Table 6-1 neglect doppler broadening of the uranium-235 fission cross section.

Recommended values of doppler coefficients for the UVAR reactor are:

1) LEU-22: -1.1×10^{-5} % $\Delta\rho$ per ^{o}C
2) LEU-18: -1.0×10^{-5} % $\Delta\rho$ per ^{o}C
3) HEU-18: -1.3×10^{-6} % $\Delta\rho$ per ^{o}C

As estimated absolute error of 10 percent is believed to be associated with each of the above values.

6.1.2 Moderator Temperature Effects

Moderator temperature effects were determined by adjusting the moderator temperature parameter of the LEOPARD code. Table 6.2 presents reactivity worths and moderator temperature coefficients for the UVAR core. Reactivity worths were calculated based on changes in k-effective relative to the reference case (moderator temperature = 21^{o}C).

Moderator temperature coefficients are relatively stable over the temperature range of interest and do not vary significantly between fuel types. Recommended moderator temperature coefficients for the UVAR are the values presented for the 50^oC case for the 4-by-5 core because the UVAR normally operates with moderator temperatures below 50^oC. An estimated 10% absolute error is considered appropriate for the recommended coefficients.

Table 6.2 Moderator Temperature Effects for the UVAR Reactor

Moderator Temperature (^oC)	Reactivity Worth ($\Delta\rho$)	Moderator Temperature Coeff ($\Delta\rho$ per ^oC)
I. UVAR 4-by-4 Core Configuration (1988 Study)		
	LEU-22 Fuel	
50	-5.0×10^{-3}	-1.7×10^{-4}
75	-1.1×10^{-2}	-2.0×10^{-4}
	LEU-18 Fuel	
50	-5.3×10^{-3}	-1.8×10^{-4}
75	-1.1×10^{-2}	-2.0×10^{-4}
	HEU-18 Fuel	
50	-5.4×10^{-3}	-1.8×10^{-4}
75	-1.1×10^{-2}	-2.0×10^{-4}
II. UVAR 4-by-5 Core Configuration (1989 Study)		
	LEU-22 Fuel	
50	-3.9×10^{-3}	-1.4×10^{-4}
75	-8.5×10^{-3}	-1.6×10^{-4}
95	-1.3×10^{-2}	-1.7×10^{-4}
	HEU-18 Fuel	
50	-4.2×10^{-3}	-1.5×10^{-4}
75	-8.8×10^{-3}	-1.6×10^{-4}
95	-1.3×10^{-2}	-1.8×10^{-4}

6.1.3 Power Defects

The power defect of reactivity is defined as the change in reactivity associated with bringing the reactor from a "cold" zero power condition to normal ("hot") operating temperatures. The UVAR coolant temperature rise across the core at 2 megawatts is about 7.2°C (13°F). The power defect for the UVAR was determined by first calculating the reactivity associated with a "cold" core in which the temperature of the core components and moderator were set at 17.4°C. This reactivity was compared with the reactivity of a "hot" core where the average moderator temperature was 21°C.

The power defects calculated for the 4-by-4 core configuration for the various fuel options are presented in Table 6.3.

Table 6.3. Power Defects For 4-by-4 UVAR Cores

Fuel Option	$\Delta\rho$
LEU-22	-6.8×10^{-4}
LEU-18	-7.3×10^{-4}
HEU-18	-7.6×10^{-4}

Absolute errors of the order of 5 to 10 percent are considered appropriate for the calculated power defect reactivities.

6.1.4 Gross System Heating Effects

Reactivity effects associated with gross system heating have been determined for a 20^{o}C rise in all reactor components and moderator. This is consistent with actual operating conditions on hot humid days when the bulk temperature of the pool can swing from 68^{o}F (20^{o}C) to 104^{o}F (40^{o}C) during a single day of operation. Gross system heating coefficients are presented below for the 4-by-5 core configuration with LEU-22 and HEU-18 fuel.

Fuel Type	Temperature Coeff ($\Delta\rho/^{o}C$)
LEU-22	-1.11×10^{-4}
HEU-18	-1.13×10^{-4}

The gross system heating coefficients for each fuel type are similar and have an estimated absolute error of about 10 percent.

6.2 Moderator Void Effects

6.2.1 Uniform Core Void Effects

Uniform moderator void effects on core reactivity, and void coefficients, have been determined for UVAR 4-by-5 graphite reflected cores with LEU-22, LEU-18, and HEU-18 fuel loadings. Uniform moderator voids ranging from 1 to 95 percent were analyzed.

Uniform voids in the core-moderator region were simulated by adjusting core water densities in the LEOPARD fuel and control rod element models. Cross sections generated by the LEOPARD code were then used in the 2DB diffusion theory code eigenvalue calculation. Reactivity worths ($\Delta\rho$) associated with uniform core voids were determined by the change in k-effective relative to the no-void core condition.

Table 6.4 presents reactivity worths associated with different void fractions for LEU-22, LEU-18 and HEU-18 fuels. The core moderator densities used to simulate the uniform core voids are also presented.

Table 6.4 Reactivity Effects Associated With Uniform Moderator Void Conditions With LEU-22, LEU-18, and HEU-18 Fuel Loadings.

% Void	Moderator Density(g/cm^3)	LEU-22 (%$\Delta\rho$)	LEU-18 (%$\Delta\rho$)	HEU-18 (%$\Delta\rho$)
1	0.99	-0.193	-0.173	-0.152
2	0.98	-0.386	-0.348	-0.307
5	0.95	-1.16	-1.00	-0.887
10	0.90	-2.48	-2.18	-1.94
20	0.80	-5.77	-5.16	-4.66
50	0.50	-24.7	23.3	-24.3
90	0.10	-150.	-161.	-165.
95	0.05	-211.	-236.	-253.

Uniform moderator void coefficients were determined by dividing the reactivity worths presented in Table 6.4 by their associated percent void. Void coefficients calculated in this manner are presented in Table 6.5.

Table 6.5 Uniform Moderator Void Coefficients for LEU-22, LEU-18, and HEU-18 Fuels.

	Void Coefficient		
% Void	LEU-22	LEU-18	HEU-18
1	-0.193	[illegible]	[illegible]
2	-0.193	[illegible]	[illegible]
5	-0.231	[illegible]	[illegible]
10	-0.248	-0.216	-0.194
20	-0.289	-0.258	-0.233
50	-0.493	-0.466	-0.486
90	-1.67	-1.79	-1.83
95	-2.2[illegible]	-2.48	-2.66

Figure 6-1 presents a plot of the void coefficient versus percent void for each fuel option.

Information provided above shows that in the 1 to 20 percent void region, the void coefficient for the LEU-18 fuel is higher than in the HEU-18 fuel. This is as expected because the harder flu[illegible] associated with LEU fuel is more sensitive to mo[illegible] changes. Similarly, void coefficients for LEU-22 fuel are higher than for LEU-18 fuel due to the smaller water gaps associated with LEU-22 (and consequently a harder spectrum).

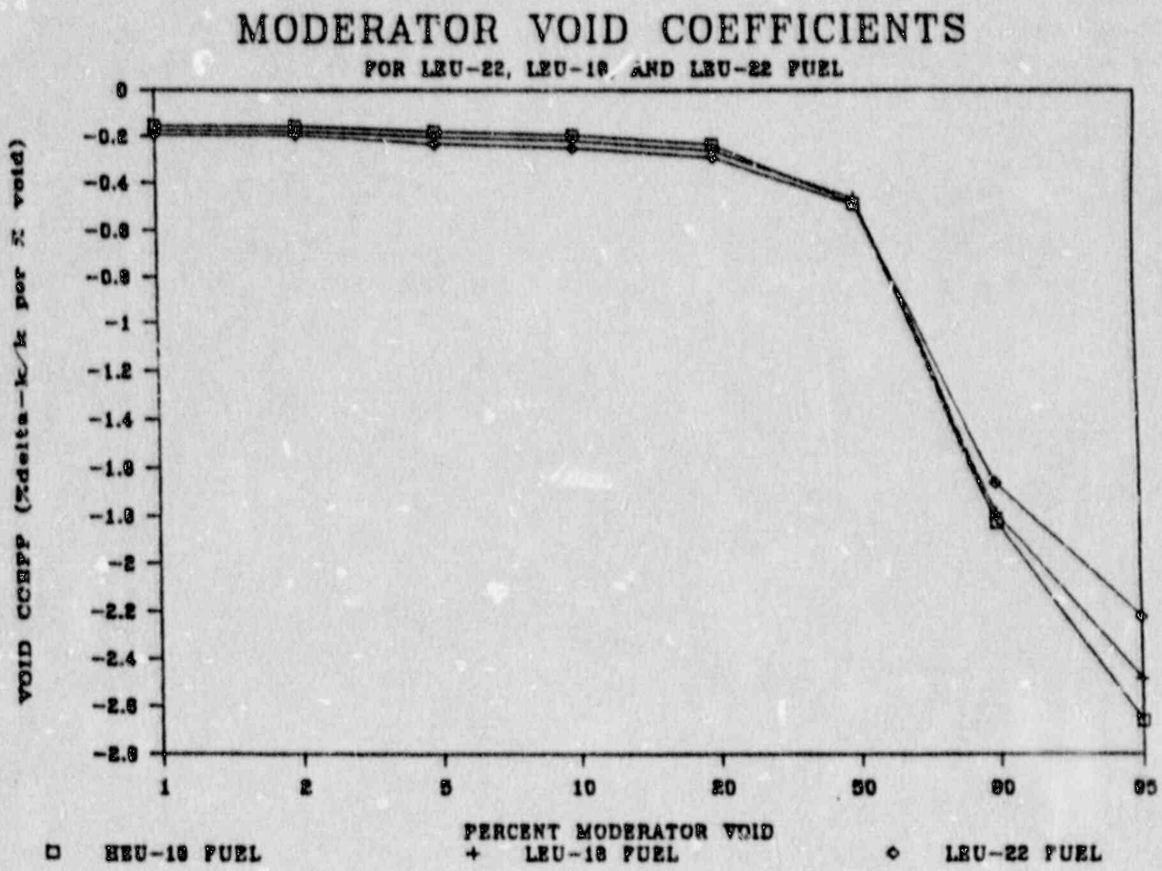

Figure 6-1. Void Coefficient As A Function Of Void Percent

A 20 percent total core void is significant and is considered a reasonable upper limit for void-effect studies. Void effects in this analysis were also considered for higher void fractions of 50, 90 and 95 percent. It should be noted that analyzing these higher void fractions "pushes" our current neutronics computer modeling capabilities due to limited data libraries and the breakdown of diffusion theory with increasing void fractions. Therefore, results presented above for the higher void fractions are not considered rigorous but are presented to provide insight into the general nature of void effects in severely voided cores.

6.2.2 Local Core Void Effects

Local void effects were analyzed for a UVAR 4-by-5 graphite reflected core with LEU-22, LEU-18, and HEU-18 fuels. Local void effects were determined by voiding 99 percent of the core moderator in local fuel element regions. As mentioned earlier, severe void conditions are difficult to model with diffusion theory modeling techniques. On the othe hand, neutrons that stream across a local void are not lost to the system, so that the predicted void effects may indeed be meaningful.

Four different local void scenarios were considered. Each scenario consists of voiding 99 percent of the core moderator in particular regions. The locations of the voided regions (see Figure 3-2) considered are as follows:

Scenario 1 - West region of Element 11.

Scenario 2 - East regions of Elements 10 and 6, and West regions of Elements 11 and 7.

Scenario 3 - West region of Element 11 and entire Element 10 fuel region.

Scenario 4 - Fuel regions of Elements 10, 11, 6, and 7.

Each scenario includes voiding the west region of Element 11. This is where the "hot-channel" is located (determined by the Peaking Factor study in Chapter 5) and is therefore the most likely region to void.

Table 6.6 presents reactivity effects associated with the different void cases for LEU-22, LEU-18, and HEU-18 fuels. Reactivity worths are calculated relative to the unvoided core.

Table 6.6 Local Void Reactivity Effects for Void Scenarios 1 Through 4

Case	LEU-22 (%$\Delta\rho$)	LEU-18 (%$\Delta\rho$)	HEU-18 (%$\Delta\rho$)
1	-0.678	-0.730	-0.834
2	-2.88	-3.16	-3.59
3	-3.49	-3.77	-4.23
4	-8.67	-9.50	-10.7

Unlike the uniform-moderator void effects discussed in Section 1, local void reactivity effects appear to be greater for the HEU fuel option which has a softer spectrum.

Local void coefficients have been developed by dividing the reactivity worths presented in Table 6.6 by the percent core water void. The percent core water void represents the ratio of the void volume to the total moderator volume of the unvoided core. Table 6.7 presents local void coefficient and percent core voids associated with each scenario for LEU-22, LEU-18, and HEU-18 fuel.

Table 6.7 Local Moderator Void Coefficients (%$\Delta\rho$/% void)

Scenario	% of Core Voided	LEU-22	LEU-18	HEU-18
1	1.3	-0.52	-0.56	-0.64
2	4.6	-0.63	-0.69	-0.78
3	5.9	-0.59	-0.64	-0.72
4	14	-0.62	-0.68	-0.76

Local moderator void coefficients appear to be relatively constant over the scenarios considered. Unlike the uniform void cases, higher void coefficients were consistently determined for the HEU soft-spectrum fuel option because these voids occurred in regions of high importance.

6.3 Temperature and Moderator Effects Summary

Temperature and moderator effects were analyzed for the UVAR reactor. Based on the results presented above, the following summary statements can be made.

1. Doppler effects in the LEU fuel were found to be about an order of magnitude greater than in the HEU fuel due to the higher U-238 loading.
2. Moderator temperature coefficients were about the same for the different fuel types and were larger than the doppler coefficients by an order of magnitude for the LEU fuel and by two orders of magnitude for the HEU fuel.
3. The power defects and gross system heating effects calculated for the different fuel types were similar to each other and appeared to be dominated by moderator temperature effects.
4. Uniform moderator void coefficients were slightly higher in the LEU fuels than in the HEU fuel due to harder flux spectra as expected. This trend faltered as void fractions were increased past 50 percent.
5. Local moderator void coefficients appear to be relatively constant for the various scenarios and, unlike the uniform void coefficients, higher coefficients were found for the soft-flux spectrum cases (HEU-18) than for the LEU cases.

CHAPTER 7.0 REFLECTOR WORTH STUDY

Reflector worths were determined for several different reflector materials and thicknesses placed on different faces of the UVAR reactor in a 4-by-5 core configuration. Reflector materials analyzed include graphite, water, deuterium tanks, and black boundaries (total absorbers). LEU-22, LEU-18, and HEU-18 fuel options were considered. The results of this study were first presented via a UVA internal memorandum [28]. Due to model revisions incorporated after the completion of that study, reflector worths presented here have an estimated uncertainty of approximately 10 percent.

7.1 Graphite And Water Reflector Options

The UVAR reactor fuel and control rod elements are positioned on the UVAR grid plate, which has an 8-by-8 array of grid locations. Grid locations may be occupied by a fuel element, control rod fuel element, graphite element, or grid plug.

For the purposes of this analysis, the 4-by-5 core configuration was assumed to be centrally located on the grid plate. Remaining grid locations, surrounding the core, were assumed to contain either graphite elements or grid plugs. Grid plugs are short devices that do not extend into the active fuel region of the core, thus a grid location with a grid plug provides pool water reflector for the core in that location. The entire grid plate assembly is, of course, surrounded by pool water.

Several different reflector options were developed using graphite and water reflectors. Reflector Options 1 through 6 are variations of a full graphite reflector as shown in Figure 7.1.

Option 1 consists of two full rows of graphite on the north, west, and east core faces, and a single row of graphite on the south core face. Reflector Options 2 through 6 were created by replacing graphite with water reflector on one or more of the core faces. Option 7, shown in Figure 7.2, consists of a single row of graphite surrounding the core. Options 8 through 12 are variations of Option 7 as shown in Figure 7.2. Option 13 (not shown) is the all-water reflector option. Reactivity worths associated with Options 2 through 6, and Options 7 and 13, calculated relative to Option 1, are presented in Table 7.1.

The reactivity worth associated with going from a full graphite reflector (Option 1) to a single row of graphite surrounding the core (Option 7) is only about 1.5%, while the reactivity swing from Option 1 to the full water reflector (Option 13) is over 7 percent. This shows that the importance of the first row of graphite reflector far outweighs the outermost second row.

Table 7.2 presents reactivity effects associated with Options 8 through 13. Reactivity worths are calculated relative to Option 7.

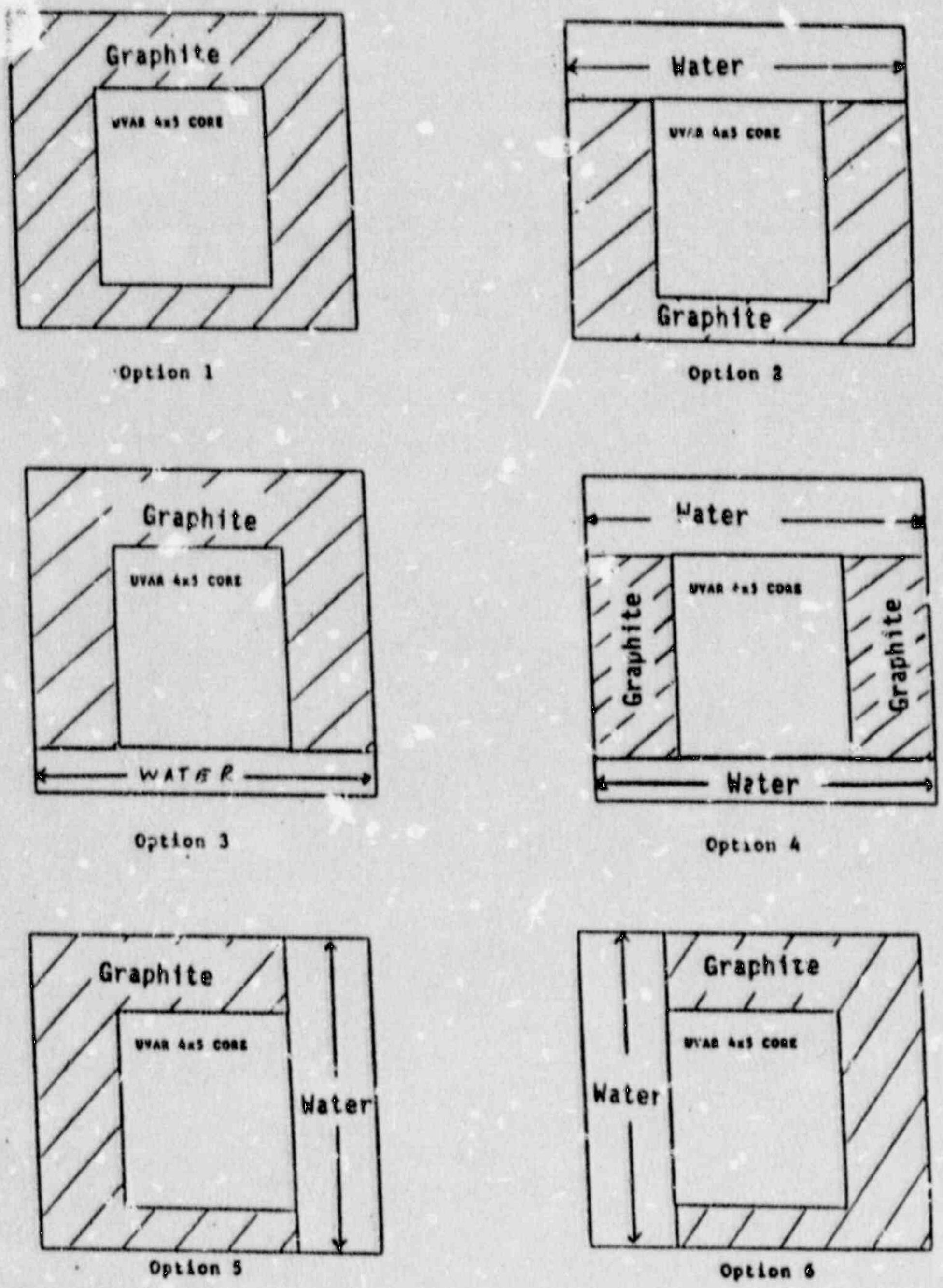

Figure 7-1. Reflector Options 1 through 6.

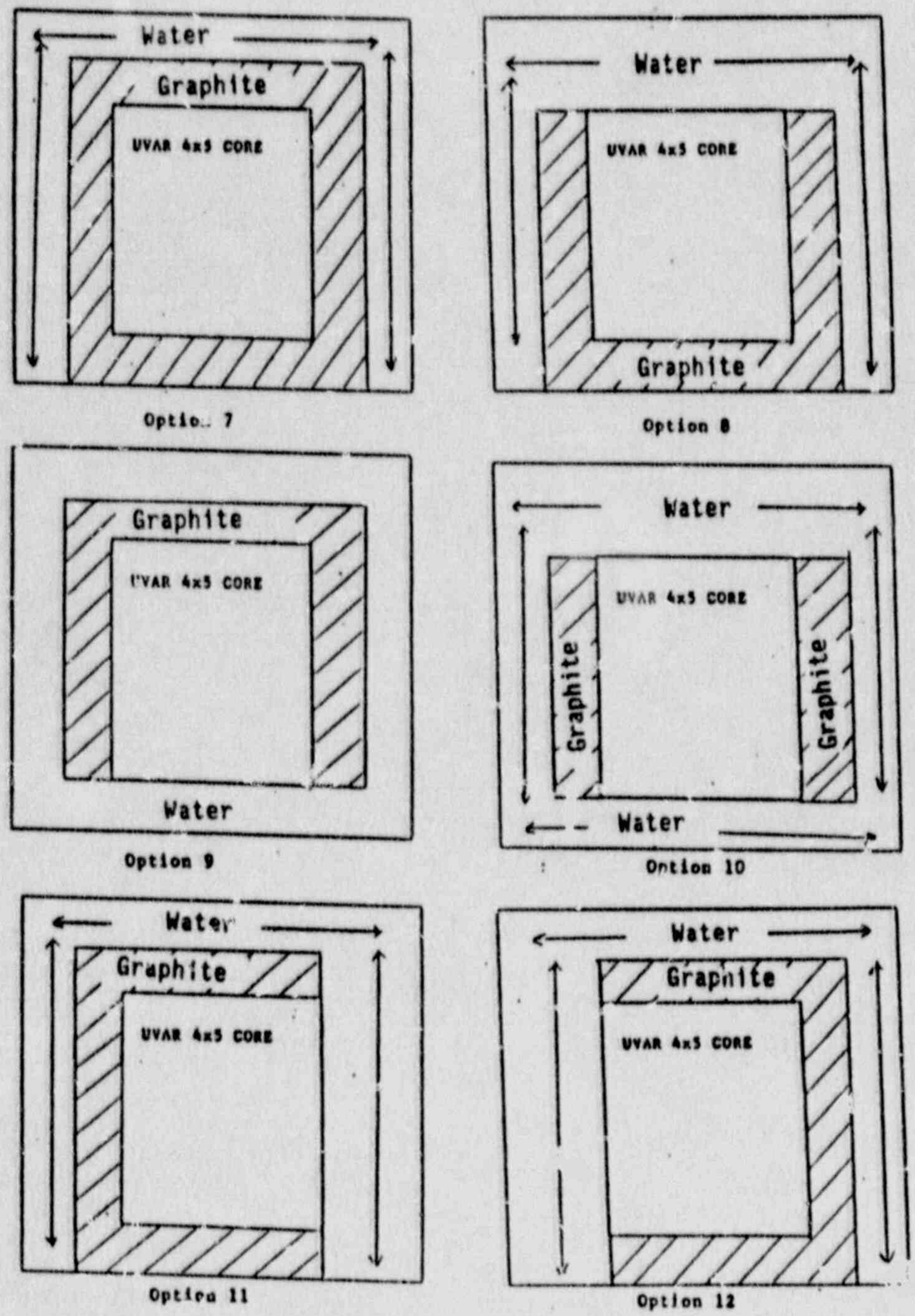

Figure 7-2. Reflector Options 7 through 12.

Table 7.1. Reactivity Effects Associated With Variations Of A Full Graphite Reflected 4-by-5 Core

Option	Reflector Description	LEU 18 FUEL (%Δρ)*	LEU-22 FUEL (%Δρ)*
1	Full graphite reflector: two rows of graphite on the east, north, and west face; and one row of graphite on the south face.	Reference Core	
2	Same as Option 1 with north face graphite replaced by water.	-1.96	-1.99
3	Same as Option 1 with south face graphite replaced by water.	-1.17	-1.24
4	Same as Option 1 with north and south face graphite replaced by water.	-3.35	-3.45
5	Same as Option 1 with east face graphite replaced by water.	-2.27	-2.33
6	Same as Option 1 with west face graphite replaced by water.	-2.19	-2.28
7	Single row of graphite surrounding entire core.	-1.48	-1.55
13	All-water reflector.	-7.23	-7.42

*Reactivity worths calculated relative to Option 1.

Table 7.2 Reactivity Effects Associated With Variations Of A Single Graphite Reflector Row Surrounding the 4-by-5 Core.

Option	Reflector Description	LEU 18 FUEL (%Δρ)*	LEU-22 FUEL (%Δρ)*
7	Single row of graphite surrounding entire core.	Reference Core	
8	Same as Option 7 with north face graphite replaced by water.	-1.36	-1.38
9	Same as Option 7 with south face graphite replaced by water.	-1.12	-1.18
10	Same as Option 7 with north and south face graphite replaced by water.	-2.64	-2.71
11	Same as Option 7 with east face graphite replaced by water.	-1.74	-1.78
12	Same as Option 7 with west face graphite replaced by water.	-1.69	-1.74
13	All-water reflector.	-5.75	-5.87

*Reactivity worths calculated relative to Option 7.

Information in Tables 7.1 and 7.2 shows that reflector reactivity effects are slightly greater for LEU-22 fuel than for LEU-18 fuel due to the harder leakage spectrum of the latter.

The effect of burnup on the relative worth of a reflector variant was determined for Option 2 using LEU-18 fuel. Four time steps were considered ranging from 0 to 384 megawatt-days. The results of this analysis show that the relative worth increases on the order of 10 percent over core life. Reflector worth increases with burnup because as the core burns, the flux shape is flattened resulting in higher leakage. These results are considered to be representative of the behavior of reflector worths with burnup in general. The results of the analysis are shown in Table 7.3.

Table 7.3 Core-Life Effects On Relative Worth of Reflector Option 2 Using LEU-18 Fuel.

Core Burnup Status	Relative Worth $\Delta\rho$
0 Mw-days	-1.96%
4 Mw-days	-2.02%
194 Mw-days	-2.09%
394 MW-days	-2.16%

7.2 Deuterium Reflector Tanks

Reactivity effects associated with various-sized deuterium tanks were analyzed in response to current plans to install an experimental D_2O tank between the core and the neutron beamport facilities. Preliminary designs have not yet been developed, so a wide range of D_2O tank sizes were analyzed. All D_2O tanks were assumed to be fabricated of one-quarter inch pure aluminum plate. Two group microscopic cross sections were developed for each tank using the GAMTEC code described in Section 3.

The tanks were assumed to be 59 cm high, consistent with the active fuel length, due to the 2-D limitations of our codes. It should be noted that the actual tank heights will probably be significantly shorter than the assumed 59 cm. Thus, results presented here are conservative. Tank sizes were consistent with integer grid plate spacings. 2-D Tank dimensions are specified in Table 7.4.

Table 7.4 Representative D_2O Tanks

D_2O Tank ID	2-D Physical Dimensions
Tank 1	8.1 cm x 7.7 cm
Tank 2	8.1 cm x 15.4 cm
Tank 3	16.2 cm x 15.4 cm
Tank 4	24.3 cm x 15.4 cm
Tank 5	24.3 cm x 23.1 cm
Tank 6	8.1 cm x 30.8 cm
Tank 7	16.2 cm x 38.5 cm
Tank 8	16.2 cm x 80.8 cm

Reflector Option 6 was used as the reference core to determine D_2O tank reactivity effects. Option 6 consists of a full graphite reflector on the north, east, and south core faces and water reflector on the west core face. Core reactivities associated with the D_2O tanks were determined by placing the tanks on the west core face (thus replacing water reflector). Table 7.5 presents reactivity worths associated with each tank.

Table 7.5 Reactivity Effects Associated With Different Sized D_2O Tanks Bordering West UVAR Core Face.

Tank	Reactivity Worth (%$\Delta\rho$)
1	0.38
2	0.77
3	0.89
4	1.4
5	1.3
6	1.4
7	1.8
8	2.1

Information presented in Table 7.5 shows that a D_2O Tank may produce a significant positive reactivity effect when replacing water reflector. To determine how this compares with graphite reflector material, graphite reflector was placed in the Tank 8 location. The reactivity associated with the graphite was 1.9% $\Delta\rho$, which is only slightly lower than the 2.1% $\Delta\rho$ associated with Tank 8. Therefore, while the D_2O tanks are significantly better reflectors than light water, they are only marginally better than graphite.

7.3 Black Boundary Reflectors

A single case, using a 4-by-5 core model with LEU-22 fuel, was analyzed with a black (vacuum) boundary on the east face of the core. The associated reactivity worth was determined to be about -8% $\Delta\rho$ relative to replacing graphite, and about -5 to -6% $\Delta\rho$ relative to replacing water. It should be noted that diffusion theory codes cannot really handle black boundaries properly so that the worths presented are only approximations that are likely to be overestimates of the true situation.

7.4 Reflector Worth Study Summary

Based on the information presented in the sections above the following summary conclusions can be made.

1. Reflector effects are slightly more pronounced in the LEU-22 fuel than in the LEU-18 fuel due to the higher leakage associated with the harder flux spectrum.
2. The calculated k-effectives associated with the BOL LEU-22 and LEU-18 full-water-reflected cores are 1.03 and 1.02 respectively. It may be reasonable to initially load the new core with a full water reflector and

subsequently add graphite with burnup, as appropriate. This should minimize core handling operations, core configuration changes and rod calibrations. It is hoped that reflector worths determined in this study will provide input for such decisions.

3. Replacing water with a D_2O tank can lead to a significant positive reactivity insertion depending on the tank size. Replacing graphite with a D_2O tank results in a relatively small positive reactivity insertion.
4. Replacing an entire core face graphite reflector with a heavily absorbent medium or vacuum results in a negative reactivity swing on the order of 8 percent.

CHAPTER 8.0 DELAYED NEUTRON AND PROMPT NEUTRON LIFETIME STUDY

Effective delayed neutron fractions and prompt neutron lifetimes have been calculated for the UVAR 4-by-5 graphite and water-reflected core models using both LEU-22 and HEU-18 fuel options. Calculation of these parameters is in response to NRC guidance received at the TRTR-88 meeting in Oregon. A summary of methodology and results are presented below.

8.1 METHODOLOGY

Effective delayed neutron fractions (βeff) and prompt neutron lifetimes (ℓ) were calculated using the EXTERMINATOR[20] 2-D diffusion theory code. A 60-by-62 x-y mesh, identical to the mesh used in the 2DB models, was used.

Four group cross sections for the core region were calculated from LEOPARD models for the fuel and control rod elements. Four group reflector cross sections for water and graphite were taken from ANL EPRI-CELL models. Composition-dependent axial buckling terms were developed based on ANL 3-D modeling of the UVAR core.

The EXTERMINATOR code requires average reciprocal velocities for each energy group. The group structure for the LEOPARD code is not explicitly defined. Fortunately, the ANL EPRI-CELL models do specify a group structure consistent with the LEOPARD code. This group structure is presented in Table 8.1.

1

IMAGE EVALUATION
TEST TARGET (MT-3)

150mm

6"

1

IMAGE EVALUATION TEST TARGET (MT-3)

150mm

6"

1

IMAGE EVALUATION TEST TARGET (MT-3)

150mm

6"

1

IMAGE EVALUATION TEST TARGET (MT-3)

150mm

6"

Table 8.1. Energy Group Structure Used for the EXTERMINATOR Analysis.

Energy Group	E-max(eV)	$<v>$ (m/s)	χ_p
1	1.0 E7	1.8 E9	0.739
2	8.2 E5	3.4 E8	0.261
3	5.5 E3	4.9 E6	0.00018
4	0.62	2.6 E5	0.0

Delayed neutron fractions used in the analysis were based on delayed neutron yields presented by Brady, et al [29] for six precursor groups. Information was available for nine and twelve precursor groups; however, EXTERMINATOR is limited to eight groups. The delayed neutron yields from Brady were normalized to a delayed neutron fraction of 0.0065. The delayed fractions (β_i) are presented in Table 8.2.

Table 8.2. Delayed Neutron Fractions

Group	% Yield		β_i
1	0.0351		0.0002282
2	0.1809		0.001176
3	0.1778		0.001156
4	0.3837		0.002494
5	0.1565		0.001017
6	0.0659		0.0004284
		Total	0.0065

8.2 MODEL VERIFICATION

The EXTERMINATOR UVAR model was verified by: 1) checking model inputs; and 2) comparing calculated k-effective values with those calculated by our existing two group 2DB models.

Both two and four energy group EXTERMINATOR models were developed for the LEU-22 fuel core. A four group EXTERMINATOR model for HEU-18 fuel was also developed. Table 8.3 presents a comparison of k-effective values calculated by the EXTERMINATOR and 2DB codes. As stated earlier, the model core is a 4-by-5 graphite reflected core.

Table 8.3. Comparison of k-effective Values Calculated By the EXTERMINATOR and 2DB Codes.

Model	k-eff EXTERMINATOR	k-eff 2DB
1. 4 Group LEU-22	1.115	-
2 Group LEU-22	1.110	1.109
2. 4 Group HEU-18	1.118	-
2 Group HEU-18	-	1.115

Information provided in Table 8.3 shows that the EXTERMINATOR and 2DB calculated values of k-effective agree closely. This provides confidence that the EXTERMINATOR models are properly set up.

8.3 PROMPT NEUTRON LIFETIMES

Prompt neutron lifetimes were calculated by the EXTERMINATOR code using first-order perturbation theory. The prompt neutron lifetime is the weighted integral time that the average neutron lives before being captured or leaked from the core. EXTERMINATOR computes the prompt neutron lifetime by numerically solving the following equation:

$$\ell = \frac{\int_{core}[\phi^*(r,E)\frac{1}{v(E)}\phi(r,E)dE]dV}{\frac{1}{k_{eff}}\int_{core}[\int_0^\infty\phi^*(r,E')\chi_p(E')dE'\int_0^\infty\nu\Sigma_f(r,E)\phi(r,E)]dV}$$

where $\phi^*(r,E)$ = adjoint flux at location r and energy E,

$\frac{1}{v(E)}$ = reciprocal neutron velocity at energy E,

$\phi(r,E)$ = neutron flux at location r and energy E,

$\chi_p(E')$ = fraction of prompt neutrons born at energy E',

ν = prompt neutron production factor for uranium-235, and

$\Sigma_f(r,E)$ = macroscopic fission cross section at location r and energy E.

Prompt neutron lifetimes have been calculated for both LEU-22 and HEU-18 fuels. Both graphite and water reflected cores were evaluated. The prompt neutron lifetimes associated with the LEU-22 4-by-5 graphite reflected core with control rod insertion were also evaluated. The results of the prompt neutron lifetime analysis are presented in Table 8.4.

Table 8.4 shows that the prompt neutron lifetime for the LEU-22 core is about 15% lower than that of the HEU-18 core. This is as expected because of the significantly higher U-238 loading of the LEU fuel. Calculated prompt neutron lifetimes for the water reflected cores are about 20 percent lower than for the graphite reflected cores. This is due to the higher leakage and absorption associated with the water reflector.

Table 8.4. Prompt Neutron Lifetimes for the UVAR Core.

Core Description	ℓ (μsecs)
1. All-Graphite Reflector	
a) LEU-22	67.0
b) HEU-18	78.8
2. Water Reflected	
a) LEU-22	53.0
b) HEU-18	64.4
3. Graphite Reflected LEU-22 Single Rod Inserted	67.0
4. Graphite Reflected LEU-22 All Rods Inserted	66.5

Rod effects were determined by inserting two group rod cross sections into the rod hole locations. The two group cross sections were input as EXTERMINATOR groups 3 and 4. Although using two group cross sections in a 4 group model is not completely rigorous, this method does provide insight into the general behavior of prompt neutron lifetime with control rod insertion. The prompt neutron lifetime is not significantly affected by rod insertion.

8.4 EFFECTIVE DELAYED NEUTRON FRACTIONS

The EXTERMINATOR code calculates effective delayed neutron fractions based on input delayed-group neutron energy spectra. The effective delayed neutron fraction represents the importance weighted production rate of delayed neutrons divided by the total importance weighted production rate of all neutrons. The EXTERMINATOR code computes the delayed neutron fraction using the following equation:

$$\beta_{eff} = \sum_{i=1}^{6} \frac{\int_{core}[\int_0^\infty \chi_{di}(E')\phi^*(r,E')dE'\int_0^\infty \beta_i \nu\Sigma_f(r,E)\phi(r,E)dE]dV}{\int_{core}[\int_0^\infty \chi_p(E')\phi^*(r,E')dE'\int_0^\infty \nu\Sigma_f(r,E)\phi(r,E)dE]dV}$$

where $\chi_{di}(E')$ = fraction of delayed neutrons in the ith precursor group born at energy E', and

β_i = delayed neutron fraction for the ith precursor group.

Other terms in the above equation are as defined in Section 8.3.

Several references were consulted to determine the delayed neutron energy spectra. Most references (e.g. [30], [31], and [32]) agree that delayed neutrons are born at energies between 200 and 650 keV. This range is clearly bounded by EXTERMINATOR group

2 (5.5 keV to 820 keV). Duderstadt [33] presents information that implies that some delayed neutrons may be born at energies in EXTERMINATOR group 1. In order to check the sensitivity of the calculation to reasonable assumptions of the delayed neutron spectrum, the following delayed neutron spectra were evaluated:

$$\chi_1 = \begin{bmatrix} 0 \\ 1 \\ 0 \\ 0 \end{bmatrix}, \quad \chi_2 = \begin{bmatrix} 0.1 \\ 0.9 \\ 0 \\ 0 \end{bmatrix}, \quad \chi_3 = \begin{bmatrix} 0.2 \\ 0.8 \\ 0 \\ 0 \end{bmatrix}$$

The above energy spectra are believed to bound the actual situation.

Four other delayed neutron energy spectra were also evaluated to provide insight into the behavior of neutrons born at different energies. It should be noted that these spectra are not considered representative of the physical situation and were evaluated for purely academic purposes. These spectra are defined below:

$$\chi_4 = \begin{bmatrix} 1 \\ 0 \\ 0 \\ 0 \end{bmatrix}, \quad \chi_5 = \begin{bmatrix} 0 \\ 0 \\ 1 \\ 0 \end{bmatrix}, \quad \chi_6 = \begin{bmatrix} 0 \\ 0 \\ 0 \\ 1 \end{bmatrix}, \quad \chi_7 = \begin{bmatrix} 0.739 \\ 0.261 \\ 0.0002 \\ 0 \end{bmatrix}$$

The χ_1 spectrum is identical to the fission spectrum presented in Table 8.1.

Table 8.5 presents total effective delayed neutron fractions associated with each energy spectrum.

Table 8.5. Total Effective Delayed Neutron Fractions for LEU-22 Fueled Core

Energy Spectrum	βeff
1. Reasonable Spectrum Approximations	
a) χ_1	0.00736
b) χ_2	0.00724
c) χ_3	0.00713
2. "Academic" Spectrum Approximations	
a) χ_4	0.00620
b) χ_5	0.00807
c) χ_6	0.00949
c) χ_7	0.00650

The effective delayed neutron fraction appears to be relatively insensitive to reasonable spectrum approximations. A shift of about 3% is associated with allowing twenty percent of the delayed neutrons to be born in group 1. Because the χ_1 spectrum was consistently supported in the literature, it was chosen as the preferred spectrum. Based on information provided in Table 8.5, a value of $\beta eff = 0.0074$ is recommended for use with the LEU-22 fuel. An estimated absolute error of about 5% is considered appropriate; however, it should be noted that the precision is of the order of 1%.

The academic spectrum assumptions show that βeff increases as the energy of the delayed neutrons decreases, as expected. A maximum value of βeff = 0.00949 is obtained when all of the delayed neutrons are born in the thermal group. The χ_7 spectrum, which is identical to the fission spectrum (see Table 8.1), produced βeff = β = 0.0065, as expected.

To gain insight into the leakage effect, βeff was calculated for the LEU-22 fuel using an all-water reflector and a χ_1 spectrum. βeff associated with this case was 0.00752 which is about 2% higher than that calculated for the graphite-reflected case. This is reasonable considering that more prompt neutron leakage and absorption occurs with a water reflector. It should be noted that this value is well within the estimated 5% error associated with the above-recommended value of βeff.

The calculated value of βeff with a single rod inserted was 0.00738 which is not significantly different from the recommended value. The calculated value of βeff with all rods inserted is 0.00741, which is also very close to the recommended value.

Finally, βeff was calculated for the HEU-18 fuel core. The calculated value is βeff = 0.00738, which is not significantly different from the recommended value for the LEU core.

8.5 Summary of Delayed Neutron and Prompt Neutron Lifetime Study

In summary, the following conclusions have been made based on the information presented above:

1. The prompt neutron lifetime associated with the LEU-22 core is 67 μsecs, which is about 15% lower than the value calculated for the HEU core.
2. Prompt neutron lifetimes in the water reflected cores are about 20 percent lower than in the graphite reflected cores.
3. Prompt neutron lifetime is not significantly affected by control rod insertion.
4. A value of βeff = 0.0074 ± 5% is recommended for use with the LEU-22 core. Additionally, βeff appears to be relatively insensitive to reasonable assumptions in the delayed neutron spectrum.
5. The value of βeff does not change significantly with reflector options or insertion of control rods.
6. The βeff value associated with the HEU core is slightly higher, but not significantly different from the value associated with the LEU core.

9.0 CONCLUSIONS

Several key neutronics issues have been addressed by the studies presented in this thesis. Study-specific summaries have been presented with each study.

RESULTS

Control rod reactivity worths for the LEU fueled cores were found to be essentially the same as for HEU fueled cores. Control rod worths were also found to change slightly with core burn-up and core reflector changes implying the need to re-evaluate control rod worths periodically with burn-up and following reflector changes.

Peaking factors associated with LEU fuel were somewhat higher than for HEU fuel. Higher peaking factors and the relatively small water gap associated with the LEU-22 fuel have led Hosticka [4] to recommend adopting more conservative UVAR Limiting Safety System Settings.

Temperature and moderator void feedback effects for both the LEU and HEU fueled cores were found to be very similar except for the doppler effect which was significantly higher in the LEU fuel due to the higher uranium-238 loading.

Reflector worths for several different water and graphite reflector options were quantified for the LEU fueled cores. The reactivity worths of deuterium tank reflectors were found to be similar to graphite reflectors.

An effective delayed neutron fraction of 0.0074 was determined for both the LEU and HEU fueled cores. A prompt neutron lifetime of 67 micro-seconds was determined for the LEU fueled core which was about 15 percent lower than in the HEU fueled core.

CONCLUSION AND FUTURE WORK

The overall study results show that the LEU-fueled core will behave very similarly to the HEU core currently being used.

Future work on the project will include preparation and submission of a revised Safety Analysis Report and UVAR Technical Specifications to NRC, plus responding to NRC licensing concerns.

After the license renewal process is complete, an experimental data collection phase is envisioned for the initially loaded LEU core. Experimental data collected during this phase will provide information needed to "fine-tune" the UVAR neutronics models and will also address possible safety concerns such as verifying bypass flow rates, fuel element flow distributions, and radial and axial flux maps. Additional experimental data to be collected on the clean core are recommended by Meem [34].

Additional investigation of radial peaking factors using transport theory models may be useful in verifying the values presented in this thesis which were predicted by diffusion theory codes. Further investigations into the experimentally determined and calculated reactivity worth discrepancy for the regulating rod may be warranted and should include an evaluation of rod region boundary conditions. New measurements of moderator temperature coefficients and quantification of the corresponding effective core temperature rise are also warranted.

REFERENCES

1. Rydin, R.A., D. Freeman, M. Fehr, B. Hosticka, R. Mulder, Conversion of the University of Virginia Reactor to Low Enrichment Fuel, Second Year Progress Report, University of Virginia Department of Nuclear Engineering and Engineering Physics, February, 1989.

2. Fehr, M.K., Design Optimization of a Low Enrichment University of Virginia Nuclear Reactor, Masters Thesis, University of Virginia, School of Engineering and Applied Science, January 1989.

3. Freeman, D., QA Package For Control Rod Worth, Shutdown Margin and Excess Reactivity Study, Draft 3, University of Virginia Internal Report, August 9, 1988.

4. Hosticka, B., "Thermal and Hydraulic Analysis of LEU-18 and 22 Plate Fuel" Memo to the University of Virginia Reactor Safety Committee, October, 1988.

5. UVAR Design and Analysis Handbook, University of Virginia Department of Nuclear Engineering and Engineering Physics, Edited by J.P. Farrar, December 1983.

6. UVAR Gridplate blueprint.

7. National Organization Of Test, Research, And Training Reactors, Specification for Test Research Training Reactor LEU Silicide U3Si2 Fuel Plates,TRTR-6, Revision 4, May 20, 1988.

8. National Organization Of Test, Research, And Training Reactors, Specification for Low Enriched U Metal For Reactor Fuel Plates,TRTR-11, March 12, 1987.

9. National Organization Of Test, Research, And Training Reactors, Specification For Reactor Grade Uranium Silicide U3Si2 Powder,TRTR-14, Revision 2, July 1, 1987.

10. National Organization Of Test, Research, And Training Reactors, Specification For Aluminum Powder For Fuel Plate Core Matrix,TRTR-15, Revision 2, July 1, 1987.

11. EG&G Drawing 42264, Test Research Training Reactor LEU Fuel for UVAR 22-Plate Element, Revision B, Dec. 5, 1986.

12. Freeman, D., "Review of Literature Provided by L.K. Seymour's Letter of January 10, 1989", UVA Internal Memorandum, February 23, 1989.

13. Freeman, D., "Preliminary Design of 18 and 22 Plate Fuel Elements," Memo to the University Of Virginia Reactor Safety Committee, April 20, 1988.

14. Freeman, D., "Preliminary Design of 18 and 22 Plate LEU Control Rod Fuel Elements," Memo to the University Of Virginia Reactor Safety Committee, May 6, 1988.

15. United Nuclear Corporation, "UVAR Fuel Element" Blue Print #D-401580, July, 1969.

16. EG&G, "UVAR Control Rod Element" Blue Print #409339, October, 1978.

17. Barry, R.F., LEOPARD-A Spectrum Dependent Non-Spatial Depletion Code," WCAP-3269-26, Westinghouse Electric Corporation, September, 1963.

18. Bennett, C. L., Purcell, W. L., BRT: Battelle-Revised-Thermos, Battelle Memorial Instiute, Reactor Physics Department, June, 1970.

19. Carter, L.L., C. Richey, C. Hughey, GAMTECII: A Code for Generating Consistent Multigroup Constants Utilized in Diffusion and Transport Theory Calculations, Pacific Northwest Laboratory, March, 1965.

20. ORNL-4078, EXTERMINATOR-2: A Fortran IV Code For Solving Multigroup Neutron Diffusion Equations In Two Dimensions, Oak Ridge National Laboratories, 1978.

21. University of Michigan, 2DB-UM APOLLO VERSION (Based largely on 2DB Code), Version #10, September, 1986.

22. Wasserman, S., Effective Diffusion Theory Cross Sections For UVAR Control Rods, Masters Thesis, University of Virginia, School of Engineering and Applied Science, June, 1989.

23. Freeman, D., "Review Documentation of S. Wasserman's Work", University of Virginia Internal Memorandum, April 12, 1988.

24. Farrar, J.P., "Results of Testing For 18 Plate Texas A&M Fuel Elements In UVAR Reactor," Letter to Nuclear Regulatory Commission, June 17, 1975.

25. Private Communications with J. Matos, Argonne National Laboratories, Winter, 1988.

26. Sternberg, H.I., Thermal Power Calculation and Correlation of UVAR by Foil Irradiation and Heat Balance, Masters Thesis, University of Virginia, November 1981.

27. Freeman, D., "Temperature and Moderator Effects for the UVAR Core." University of Virginia Internal Memorandum, May 31, 1988.

28. Freeman, D., "Reactivity Effects Associated With Various UVAR Core Reflector Options", University of Virginia Internal Memorandum, March 16, 1989.

29. Brady, M.C., R. Talmadge, W. Wilson, "Few-Group Analysis of Current Delayed Neutron Data", ANS Transactions, Volume 53, 1988.

30. Argonne National Laboratories, Reactor Physics Constants, ANL-5800, Second Edition, 1963.

31. LaMarsh, J. R., Introduction To Nuclear Reactor Theory, Addison-Wesley Publishing Company, 1965.

32. Keepin, G.R., Physics Of Nuclear Kinetics, Addison-Wesley Publishing Company, 1965.

33. Duderstadt, J.J., L.J. Hamilton, Nuclear Reactor Analysis, John Wiley and Sons, Inc., New York, 1976.

34. Meem, J.L., "Possible Experiments On the New LEU Core", Memo to University of Virginia Reactor Safety Committee, October 20, 1988.

APPENDIX A. MATERIAL CROSS SECTIONS FOR UVAR 2-D CORE MODEL

This Appendix presents material cross sections for the UVAR 2-D Core model. Tables A-1 through A-3 present core region cross sections developed with the LEOPARD code. Table A-4 presents control rod cross sections for both the safety and regulating rods using the various fuel options. Table A-5 presents ANL calculated water and graphite reflector cross sections and Table A-6 presents UVA developed graphite reflector cross sections.

Table A-1. Core Region Cross Sections for LEU-22 Fuel (cm^{-1}).

Description	Group	Σ_f	Σ_a	$\nu\Sigma_f$	Σ_{tr}	$\Sigma_{g,g}$	$\Sigma_{(g-1),g}$
I. Two Group Cross Sections							
1. Fuel Lattice	1	2.32×10^{-3}	6.22×10^{-3}	5.71×10^{-3}	2.54×10^{-1}	2.22×10^{-1}	0.0
	2	9.32×10^{-2}	1.26×10^{-1}	2.25×10^{-1}	1.26×10^{0}	1.13×10^{0}	2.57×10^{-2}
2. Fuel Non-Lattice	1	0.0	3.83×10^{-4}	0.0	1.89×10^{-1}	1.75×10^{-1}	0.0
	2	0.0	1.31×10^{-2}	0.0	6.15×10^{-1}	6.02×10^{-1}	1.38×10^{-2}
3. Control Rod Element Non-Lattice	1	0.0	4.08×10^{-4}	0.0	2.70×10^{-1}	2.32×10^{-1}	0.0
	2	0.0	1.67×10^{-2}	0.0	1.61×10^{0}	1.59×10^{0}	3.76×10^{-2}
II. Four Group Cross Sections							
1. Fuel Lattice	1	6.91×10^{-4}	1.11×10^{-3}	1.91×10^{-3}	1.68×10^{-1}	8.46×10^{-2}	0.0
	2	4.05×10^{-4}	8.83×10^{-4}	9.89×10^{-4}	3.04×10^{-1}	2.09×10^{-1}	8.21×10^{-2}
	3	6.47×10^{-3}	1.84×10^{-2}	1.57×10^{-2}	4.09×10^{-1}	3.05×10^{-1}	9.44×10^{-2}
	4	9.32×10^{-2}	1.26×10^{-1}	2.25×10^{-1}	1.26×10^{0}	1.13×10^{0}	8.57×10^{-2}
2. Fuel Non-Lattice	1	0.0	3.47×10^{-4}	0.0	1.42×10^{-1}	1.00×10^{-1}	0.0
	2	0.0	1.25×10^{-4}	0.0	2.28×10^{-1}	1.80×10^{-1}	4.15×10^{-2}
	3	0.0	7.35×10^{-4}	0.0	2.26×10^{-1}	1.79×10^{-1}	4.77×10^{-2}
	4	0.0	1.31×10^{-2}	0.0	6.15×10^{-1}	6.02×10^{-1}	4.58×10^{-2}
3. Control Rod Non-Lattice	1	0.0	3.77×10^{-4}	0.0	1.76×10^{-1}	7.69×10^{-2}	0.0
	2	0.0	3.88×10^{-5}	0.0	3.16×10^{-1}	1.93×10^{-1}	9.89×10^{-2}
	3	0.0	8.67×10^{-4}	0.0	4.77×10^{-1}	3.53×10^{-1}	1.22×10^{-1}
	4	0.0	1.67×10^{-2}	0.0	1.61×10^{0}	1.59×10^{0}	1.23×10^{-1}

Table A-2. Core Region Cross Sections For LEU-18 Fuel (cm^{-1}).

Description	Group	Σ_f	Σ_a	$\nu\Sigma_f$	Σ_{tr}	$\Sigma_{g,g}$	$\Sigma_{(g-1),g}$
I. Two Group Cross Sections							
1. Fuel Lattice	1	1.93×10^{-3}	5.41×10^{-3}	4.75×10^{-3}	2.61×10^{-1}	2.26×10^{-1}	0.0
	2	7.90×10^{-2}	1.09×10^{-1}	1.91×10^{-1}	1.40×10^{0}	1.29×10^{0}	2.92×10^{-2}
2. Fuel Non-Lattice	1	0.0	3.92×10^{-4}	0.0	1.93×10^{-1}	1.77×10^{-1}	0.0
	2	0.0	1.37×10^{-2}	0.0	6.81×10^{-1}	6.67×10^{-1}	1.51×10^{-2}
3. Control Rod Element Non-Lattice	1	0.0	4.15×10^{-4}	0.0	2.67×10^{-1}	2.29×10^{-1}	0.0
	2	0.0	1.70×10^{-2}	0.0	1.65×10^{0}	1.63×10^{0}	3.81×10^{-2}
II. Four Group Cross Sections							
1. Fuel Lattice	1	5.68×10^{-4}	9.80×10^{-4}	1.57×10^{-3}	1.71×10^{-1}	8.23×10^{-2}	0.0
	2	3.31×10^{-4}	6.87×10^{-4}	8.09×10^{-4}	3.09×10^{-1}	2.05×10^{-1}	8.76×10^{-2}
	3	5.36×10^{-3}	1.59×10^{-2}	1.30×10^{-2}	4.38×10^{-1}	3.25×10^{-1}	1.04×10^{-1}
	4	7.90×10^{-2}	1.09×10^{-1}	1.91×10^{-1}	1.40×10^{0}	1.29×10^{0}	9.65×10^{-2}
2. Fuel Non-Lattice	1	0.0	3.57×10^{-4}	0.0	1.44×10^{-1}	9.99×10^{-2}	0.0
	2	0.0	1.22×10^{-4}	0.0	2.30×10^{-1}	1.78×10^{-1}	4.34×10^{-2}
	3	0.0	7.52×10^{-4}	0.0	2.39×10^{-1}	1.89×10^{-1}	5.13×10^{-2}
	4	0.0	1.37×10^{-2}	0.0	6.81×10^{-1}	6.67×10^{-1}	4.97×10^{-2}
3. Control Rod Non-Lattice	1	0.0	3.23×10^{-4}	0.0	1.74×10^{-1}	7.59×10^{-2}	0.0
	2	0.0	3.89×10^{-5}	0.0	3.12×10^{-1}	1.89×10^{-1}	9.76×10^{-2}
	3	0.0	8.75×10^{-4}	0.0	4.79×10^{-1}	3.54×10^{-1}	1.23×10^{-1}
	4	0.0	1.70×10^{-2}	0.0	1.65×10^{0}	1.63×10^{0}	1.24×10^{-1}

Table A-3. Core Region Cross Sections for HEU-18 Fuel (cm^{-1})

Description	Group	Σ_f	Σ_a	$\nu\Sigma_f$	Σ_{tr}	$\Sigma_{g,g}$	$\Sigma_{(g-1),g}$
I. Two Group Cross Sections							
1. Fuel Lattice	1	1.60×10^{-3}	3.01×10^{-3}	3.90×10^{-3}	2.58×10^{-1}	2.42×10^{-1}	0.0
	2	6.96×10^{-2}	9.64×10^{-2}	1.68×10^{-1}	1.40×10^{0}	1.30×10^{0}	3.03×10^{-2}
2. Fuel Non-Lattice	1	0.0	3.89×10^{-4}	0.0	1.98×10^{-1}	1.81×10^{-1}	0.0
	2	0.0	1.34×10^{-2}	0.0	7.21×10^{-1}	7.08×10^{-1}	1.60×10^{-2}
3. Control Rod Element Non-Lattice	1	0.0	4.13×10^{-4}	0.0	2.58×10^{-1}	2.22×10^{-1}	0.0
	2	0.0	1.63×10^{-2}	0.0	1.50×10^{0}	1.48×10^{0}	3.47×10^{-2}
II. Four Group Cross Sections							
1. Fuel Lattice	1	2.21×10^{-4}	5.87×10^{-4}	6.02×10^{-4}	1.69×10^{-1}	8.23×10^{-2}	0.0
	2	2.85×10^{-4}	4.24×10^{-4}	6.96×10^{-4}	3.05×10^{-1}	2.02×10^{-1}	8.63×10^{-2}
	3	4.65×10^{-3}	8.68×10^{-3}	1.12×10^{-2}	4.29×10^{-1}	3.21×10^{-1}	1.03×10^{-1}
	4	6.96×10^{-2}	9.64×10^{-2}	1.68×10^{-1}	1.40×10^{0}	1.30×10^{0}	9.89×10^{-2}
2. Fuel Non-Lattice	1	0.0	3.55×10^{-4}	0.0	1.46×10^{-1}	1.00×10^{-1}	0.0
	2	0.0	1.18×10^{-4}	0.0	2.34×10^{-1}	1.80×10^{-1}	4.51×10^{-2}
	3	0.0	7.40×10^{-4}	0.0	2.52×10^{-1}	1.99×10^{-1}	5.37×10^{-2}
	4	0.0	1.34×10^{-2}	0.0	7.21×10^{-1}	7.08×10^{-1}	5.21×10^{-2}
3. Control Rod Non-Lattice	1	0.0	3.76×10^{-4}	0.0	1.69×10^{-1}	7.96×10^{-2}	0.0
	2	0.0	5.26×10^{-5}	0.0	3.01×10^{-1}	1.90×10^{-1}	8.86×10^{-2}
	3	0.0	8.55×10^{-4}	0.0	4.44×10^{-1}	3.32×10^{-1}	1.11×10^{-1}
	4	0.0	1.63×10^{-2}	0.0	1.50×10^{0}	1.48×10^{0}	1.11×10^{-1}

Table A.4 Control Rod Region Cross Sections

Rod/Fuel	Group	Σ_a	Σ_{tr}	Σ_{g-g}	$\Sigma_{(g-1)-g}$
I. Safety Rods					
1. LEU-22	1	0.0182	0.270	0.573	0.0
	2	0.0171	2.00	1.53	0.0229
2. LEU-18	1	0.0186	0.271	0.577	0.0
	2	0.166	2.05	1.57	0.0233
3. HEU-18	1	0.0178	0.270	0.573	0.0
	2	0.171	2.06	1.56	0.0229
II. Regulating Rod					
1. LEU-22	1	0.00268	0.284	0.552	0.0
	2	0.0384	1.23	1.37	0.0163
2. LEU-18	1	0.00220	0.284	0.552	0.0
	2	0.0425	1.25	1.39	0.0164
3. HEU-18	1	0.00234	0.281	0.546	0.0
	2	0.0368	1.24	1.37	0.0160

[1] g-g represents in-group scattering

[2] (g-1)-g represents one group downscatter

Table A.5. ANL Developed Water and Graphite Reflector Cross Sections (cm^{-1}).

Description	Group	Σ_a	Σ_{tr}	Σ_{g-g}	$\Sigma_{(g-1)-g}$
I. Water Reflector					
1. Two Group	1	4.58×10^{-4}	2.65×10^{-1}	8.39×10^{-1}	0.0
	2	1.97×10^{-2}	2.30×10^{0}	2.63×10^{-0}	4.91×10^{-2}
2. Four Group	1	3.60×10^{-4}	1.59×10^{-1}	2.70×10^{-1}	0.0
	2	9.68×10^{-6}	3.12×10^{-1}	8.83×10^{-1}	1.07×10^{-1}
	3	1.00×10^{-3}	5.69×10^{-1}	1.38×10^{0}	1.50×10^{-1}
	4	1.97×10^{-2}	2.30×10^{0}	2.63×10^{0}	1.48×10^{-1}
II. Graphite Reflector					
1. Two Group	1	1.06×10^{-4}	2.69×10^{-1}	3.64×10^{-1}	0.0
	2	3.28×10^{-3}	4.93×10^{-1}	5.21×10^{-1}	7.23×10^{-3}
2. Four Group	1	8.90×10^{-5}	1.44×10^{-1}	1.85×10^{-1}	0.0
	2	2.73×10^{-5}	3.06×10^{-1}	3.75×10^{-1}	3.10×10^{-2}
	3	1.75×10^{-4}	3.51×10^{-1}	4.24×10^{-1}	1.99×10^{-2}
	4	3.28×10^{-3}	4.93×10^{-1}	5.21×10^{-1}	1.58×10^{-2}

Table A.6. UVA Developed Graphite Reflector Cross Sections (cm^{-1})

Description	Group	Σ_a	Σ_{tr}	Σ_{g-g}	$\Sigma_{(g-1)-g}$
Graphite Reflector	1	1.04×10^{-4}	2.63×10^{-1}	4.26×10^{-1}	0.0
	2	3.44×10^{-3}	6.25×10^{-1}	7.26×10^{-1}	5.92×10^{-3}